Correlation of the L-mode density limit with edge collisionality

by

Andrew D. Maris[1], Cristina Rea[1], Alessandro Pau[2], Jayson Barr[3], Keith Erickson[4], Wenhui Hu[5], Robert Granetz[1], and Earl Marmar[1]

[1]Plasma Science and Fusion Center, MIT
[2]Swiss Plasma Center, EPFL
[3]General Atomics
[4]Princeton Plasma Physics Laboratory
[5]Institute of Plasma Physics, Hefei Institutes of Physical Science

Presented to

Third Technical Meeting on Plasma Disruptions and their Mitigation

3 September 2024

This work is supported by the U.S. Department of Energy, Office of Science, Office of Fusion Energy Sciences, under Award DE-SC0014264

Multi-machine database & data-driven techniques uncover reliable L-mode density limit precursor (LDL-P) risk metric [1]

- **Two-parameter scaling robustly predicts LDL across devices**

$$\nu_{*,\mathrm{edge}}\beta_{T,\mathrm{edge}}^{0.4}$$ → *good for burning plasmas!*

  - 6x fewer false positives than Greenwald fraction

- **LDL-P risk metric deployed on DIII-D & utilized for successful real-time LDL avoidance (16x)**

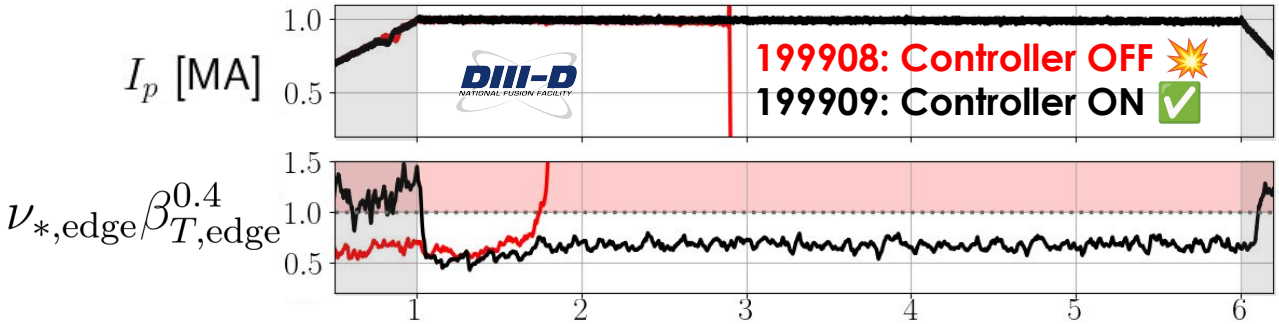

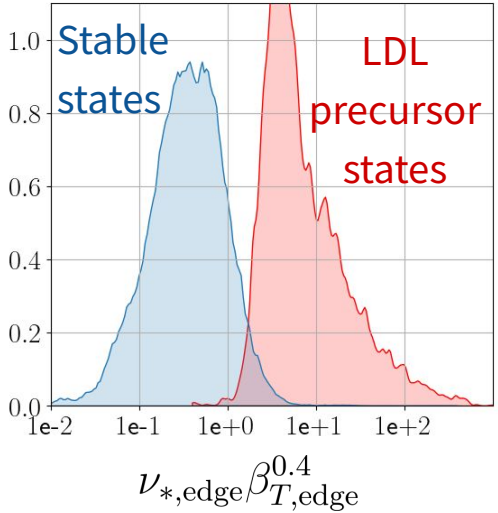

ASDEX Upgrade · Alcator C-Mod · DIII-D NATIONAL FUSION FACILITY · TCV

[1] Maris et al., *Submitted, NF* (2024)

Andrew Maris, maris@mit.edu / 2024-09-03

Outline

1. **Introduction**
2. Description of database
3. Model development
4. Real-time LDL avoidance at DIII-D
5. Summary & conclusion

Andrew Maris, maris@mit.edu / 2024-09-03

The density limit (DL) is a key limitation and risk for future tokamaks

- **High density crucial for many burning plasma scenarios**
  - Increase fusion power density (~ n^2)
  - Enable radiative divertor regimes
- **ITER & tokamak power plants set to operate near empirical Greenwald density limit [2]**

$$\frac{n}{n_G} < 1, \text{ where } n_G = \frac{I_p}{\pi a^2}$$

[2] Greenwald et al., NF (1988)
[3] Ikeda, NF (2007)
[4] Wenninger et al., NF (2015)
[5] Buttery et al., NF (2021)
[6] Sorbom et al., Fus. Eng. & Des. (2015)

Tokamak	ITER [3]	DEMO [4]	CAT [5]	ARC [6]
n/n_G	0.85	≥1	0.9-1	0.67

Andrew Maris, maris@mit.edu / 2024-09-03

Experiment and theory point to edge density and temperature as key parameters

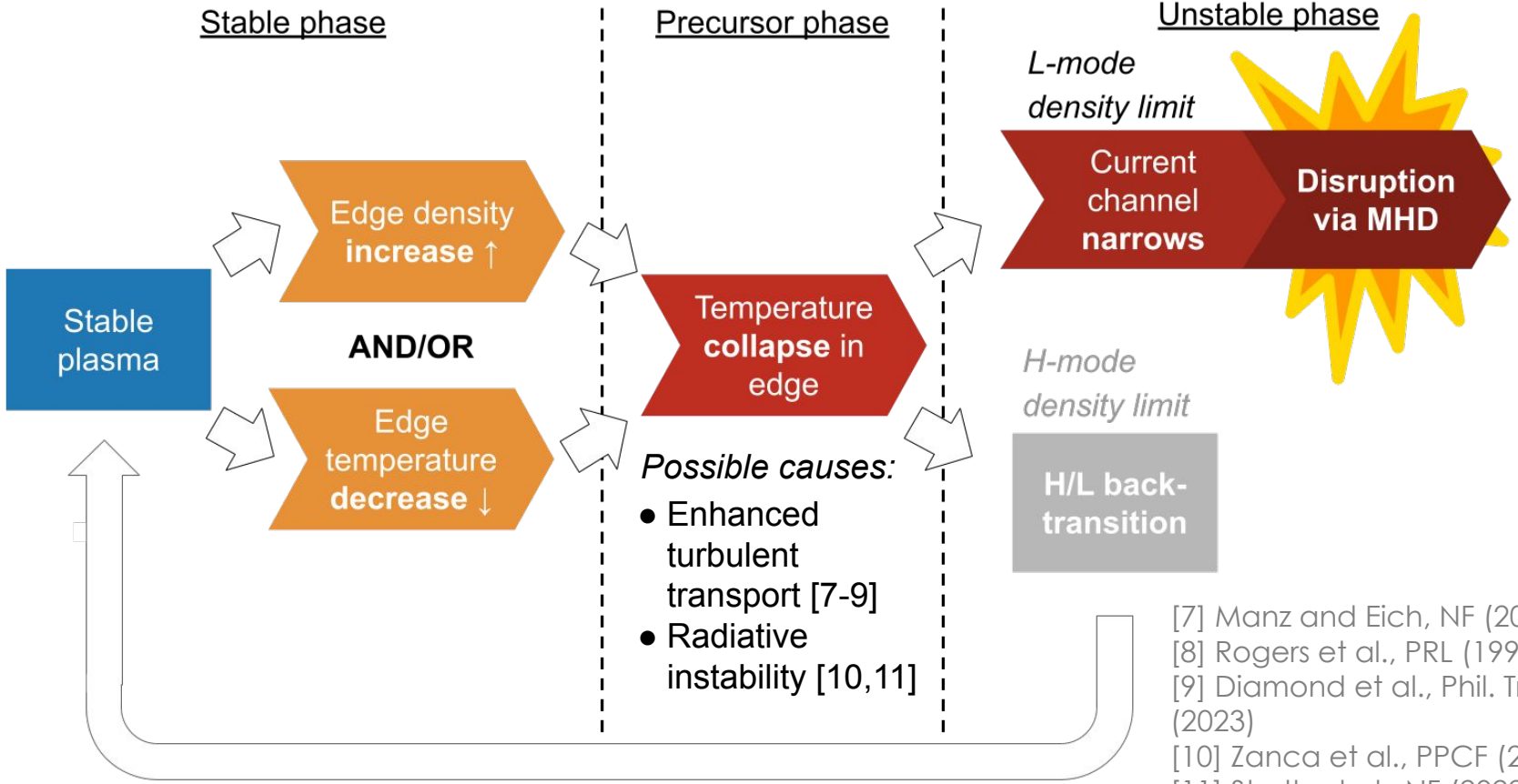

[7] Manz and Eich, NF (2023)
[8] Rogers et al., PRL (1998)
[9] Diamond et al., Phil. Trans. A. (2023)
[10] Zanca et al., PPCF (2022)
[11] Stroth et al., NF (2022)

Andrew Maris, maris@mit.edu / 2024-09-03

We focus on precursor phase as it provides early warning of LDL

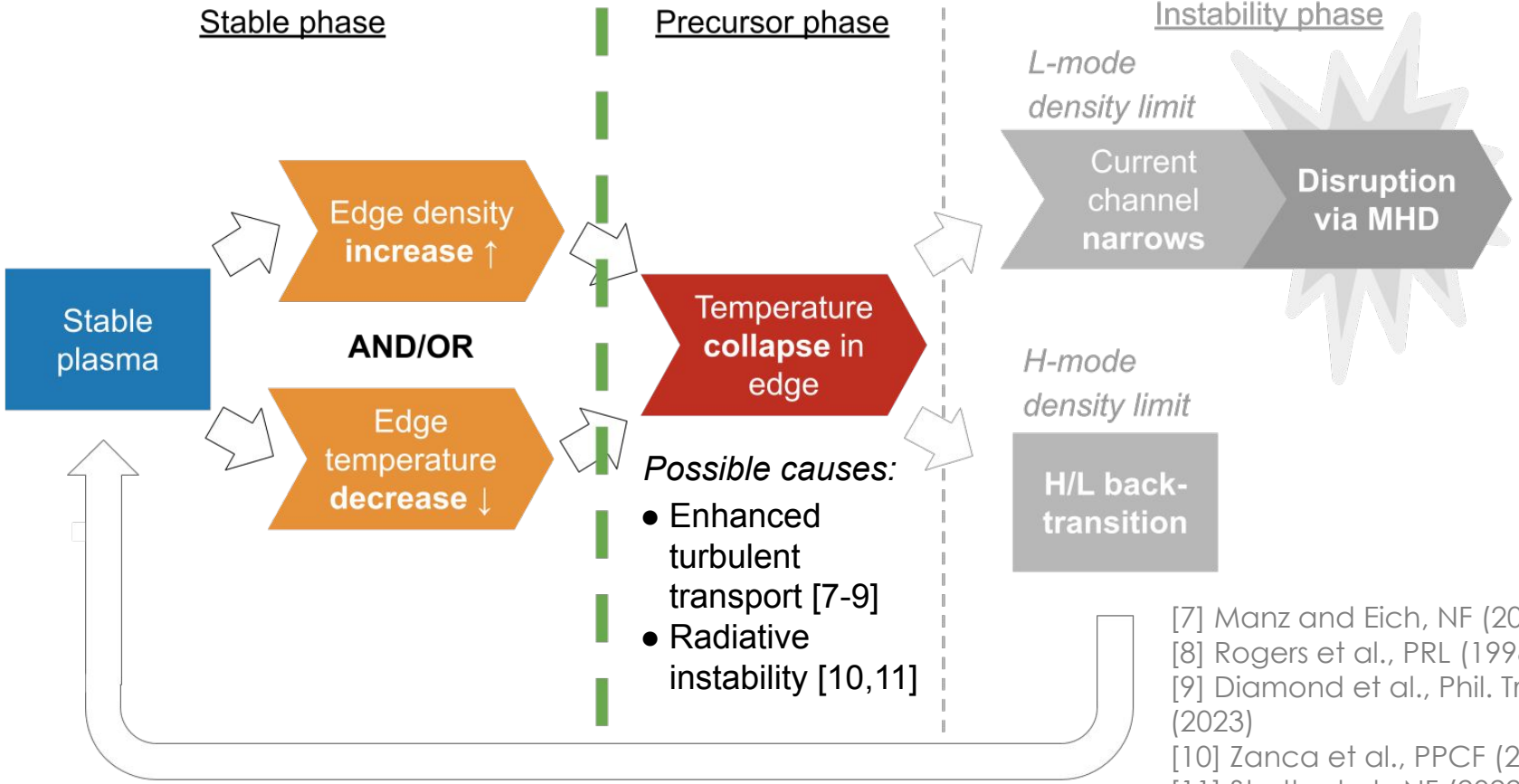

[7] Manz and Eich, NF (2023)
[8] Rogers et al., PRL (1998)
[9] Diamond et al., Phil. Trans. A. (2023)
[10] Zanca et al., PPCF (2022)
[11] Stroth et al., NF (2022)

Andrew Maris, maris@mit.edu / 2024-09-03

We focus on precursor phase as it provides early warning of LDL

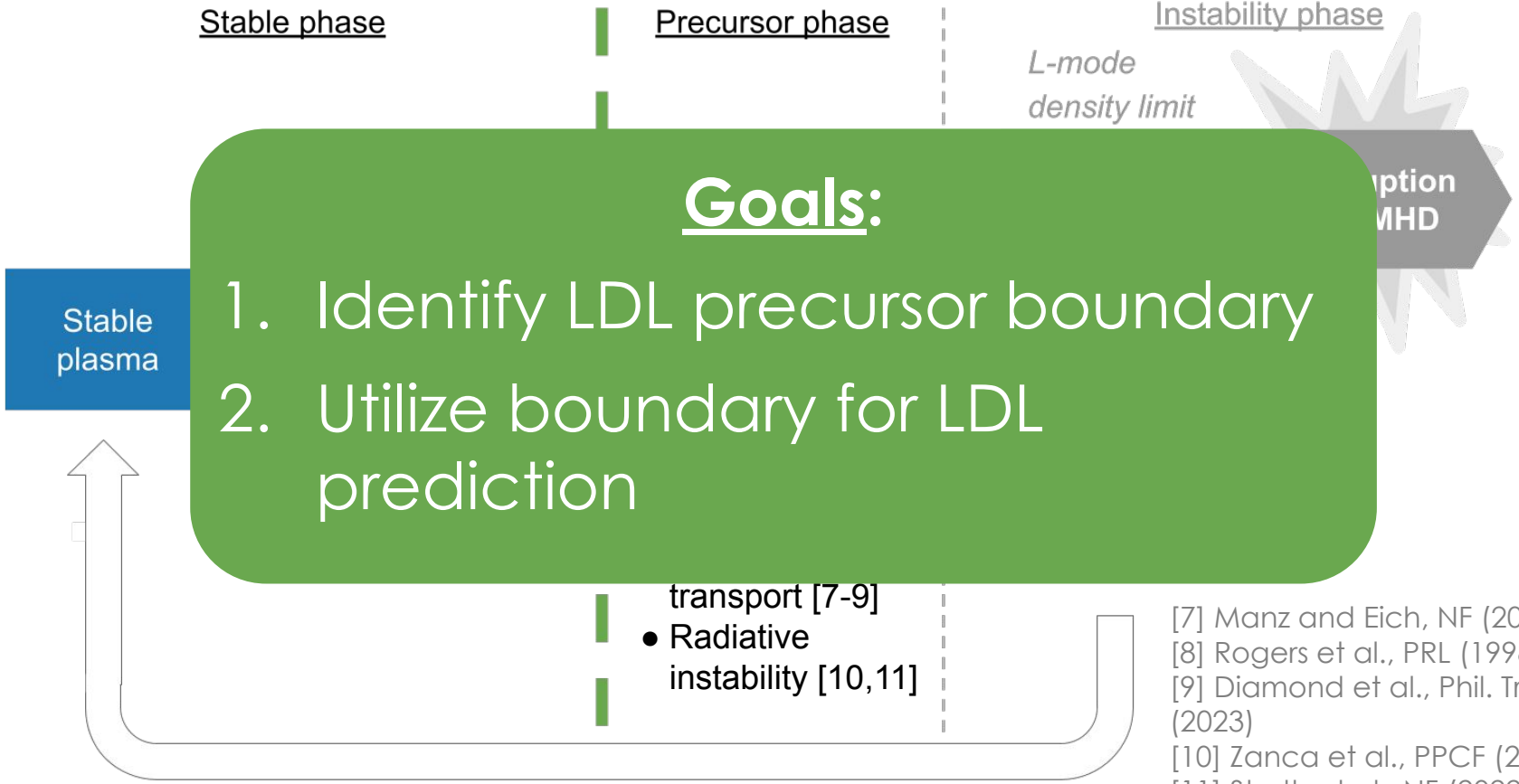

[7] Manz and Eich, NF (2023)
[8] Rogers et al., PRL (1998)
[9] Diamond et al., Phil. Trans. A. (2023)
[10] Zanca et al., PPCF (2022)
[11] Stroth et al., NF (2022)

Andrew Maris, maris@mit.edu / 2024-09-03

Outline

1. Introduction
2. **Description of database**
3. Model development
4. Real-time LDL avoidance at DIII-D
5. Summary & conclusion

We develop a database of LDL events in carbon- (DIII-D, TCV) and metal-wall (AUG, C-Mod) devices

- **Large number of LDL and non-LDL ("stable") shots**
  - # of LDL shots: 154
  - # of stable shots: 3,193
- **Significant variation in # of shots per device**

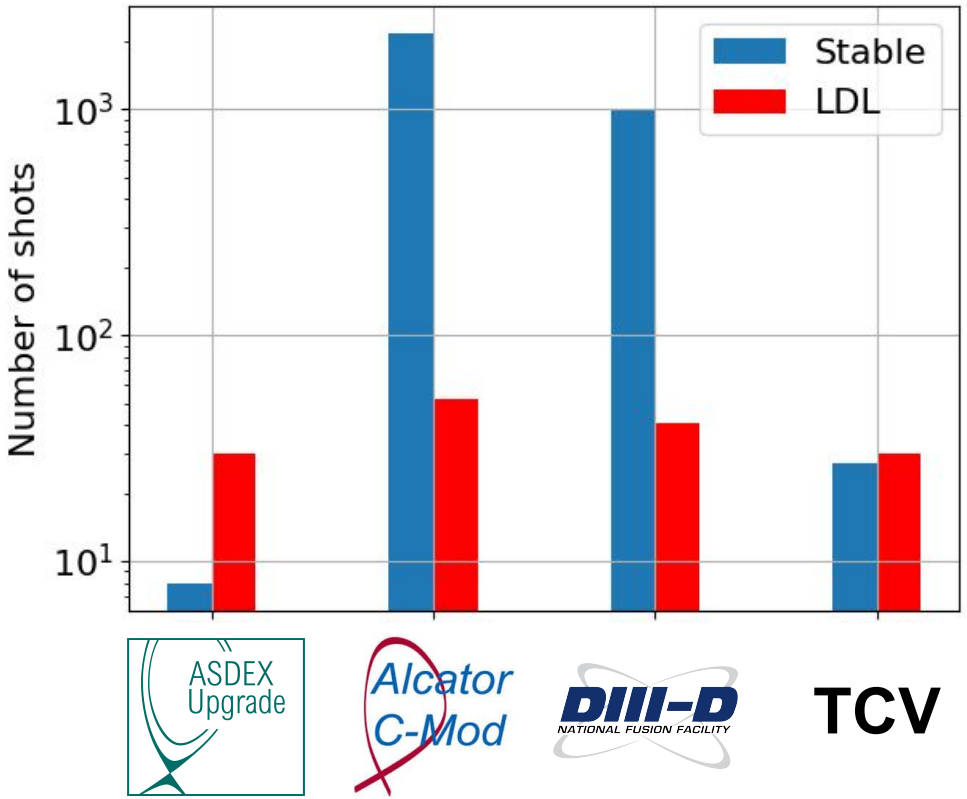

Labeling of LDL event phase done by manual inspection

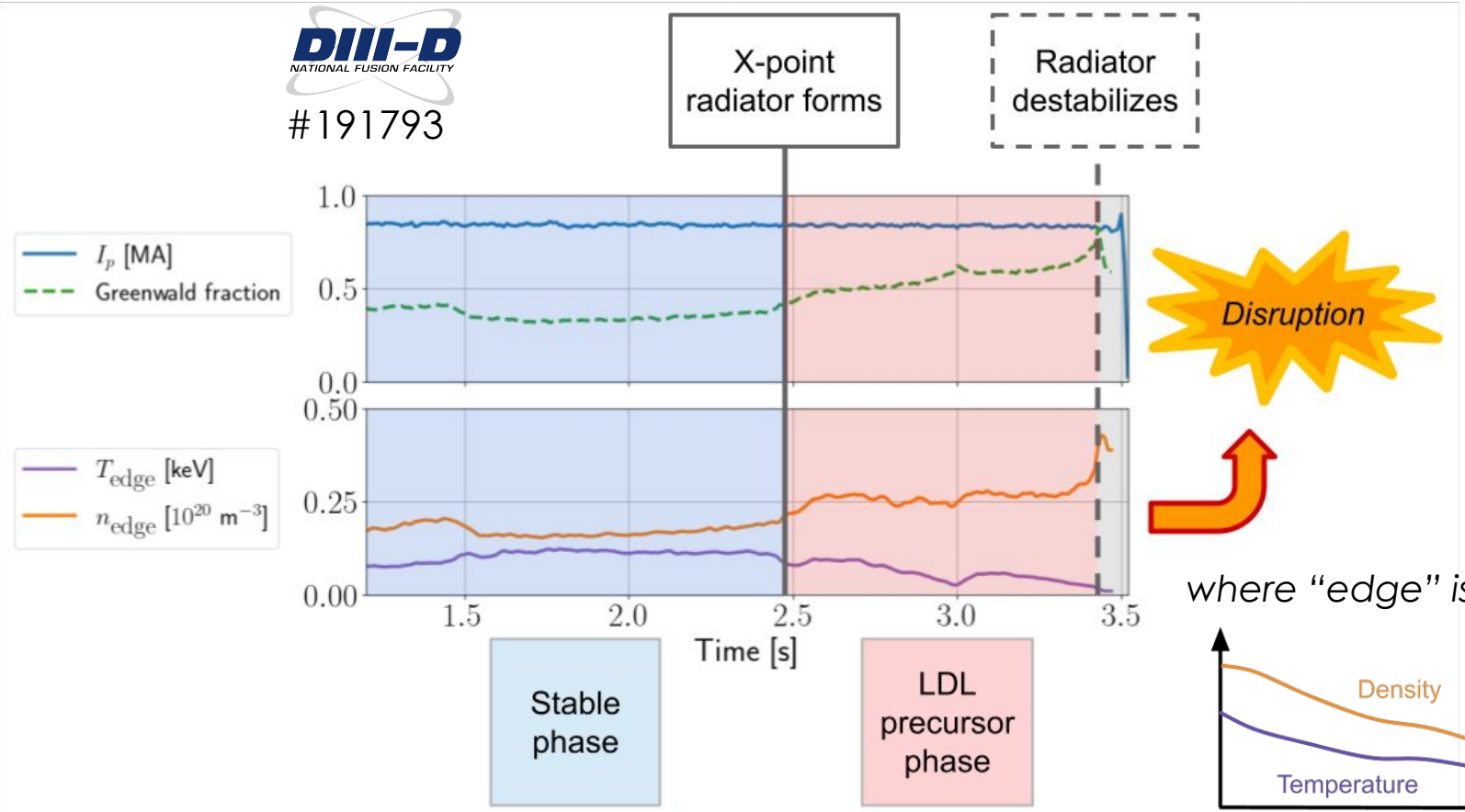

where "edge" is 0.85 < ρ < 0.95

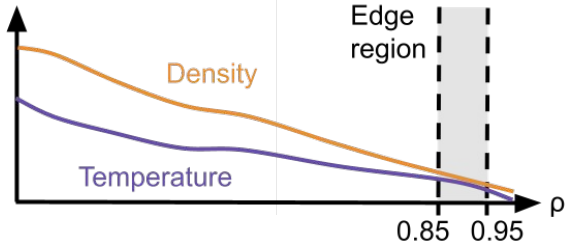

Andrew Maris, maris@mit.edu / 2024-09-03

We compare LDL stability metrics (ex. Greenwald fraction) by treating LDL prediction as binary classification problem

- **A good proximity-to-instability metric:**
  - correctly warns shot will end in LDL → high True Positive Rate (TPR)
  - rarely misclassifies stable shots → low False Positive Rate (FPR)

Andrew Maris, maris@mit.edu / 2024-09-03

We compare LDL stability metrics (ex. Greenwald fraction) by treating LDL prediction as binary classification problem

- **A good proximity-to-instability metric:**
  - correctly warns shot will end in LDL → high True Positive Rate (TPR)
  - rarely misclassifies stable shots → low False Positive Rate (FPR)
- **We can trade off between TPR and FPR by changing alarm threshold**
  - Ex. alarm threshold of $n/n_G = 1.0$ will have lower TPR and higher FPR than $n/n_G = 0.6$

Andrew Maris, maris@mit.edu / 2024-09-03

We will report two classification performance metrics

1. **"Area Under the ROC Curve" (AUC)** ∈ [0.5,1]

   → Higher is better

2. **False Positive Rate (w/ True Positive Rate = 95%)** ∈ [0,1]

   → Lower is better

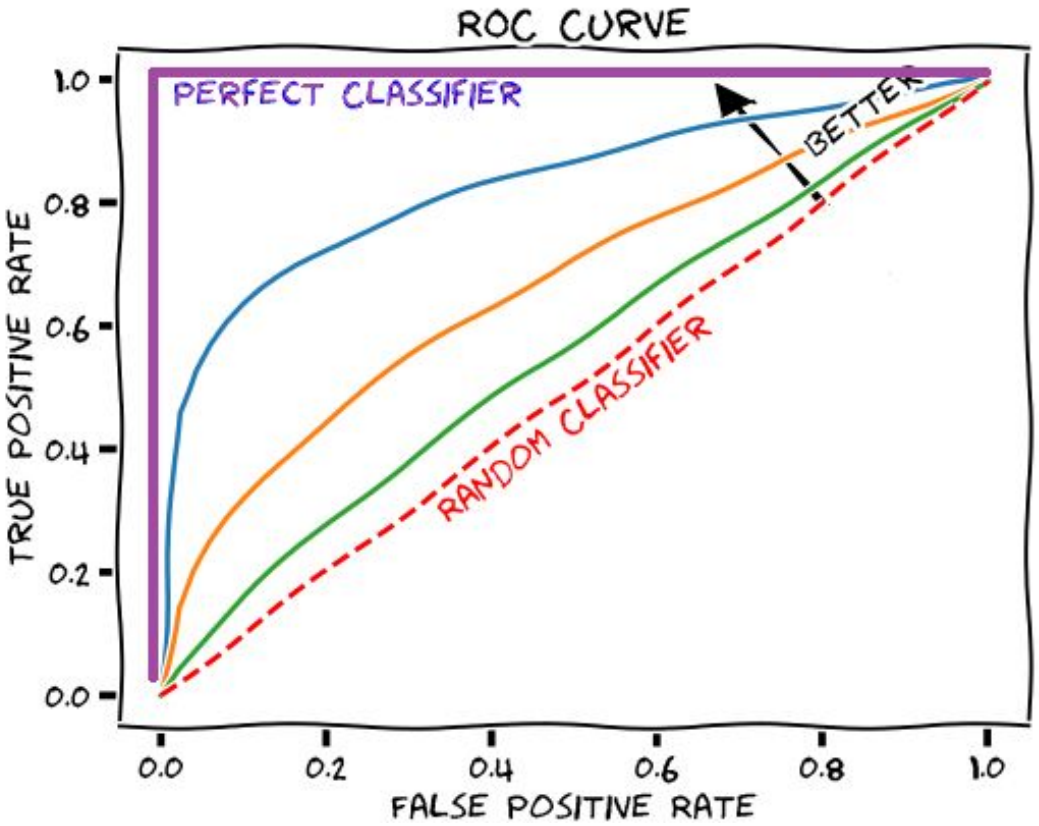

Outline

1. Introduction
2. Description of database
3. **Model development**
4. Real-time LDL avoidance at DIII-D
5. Summary & conclusion

Andrew Maris, maris@mit.edu / 2024-09-03

Greenwald fraction has some predictive power, but results in significant # of false positives

Model	Analytic boundary	AUC	FPR @ TPR = 95%
Greenwald	$\bar{n}^{\text{limit}} \sim \frac{I_p}{\pi a^2}$	0.971	13.4%

~13% False Positive Rate for a single instability would be impediment for ITER!

We use three strategies to find an LDL boundary with higher classification accuracy

1) Use classification algorithm (not linear regression!)

2) Train model to identify precursor phase

3) Utilize edge density and temperature

Linear Support Vector Machine (LSVM)

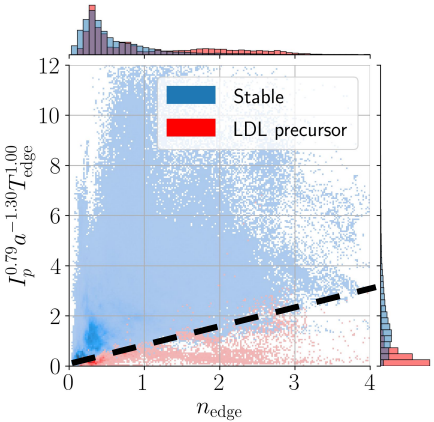

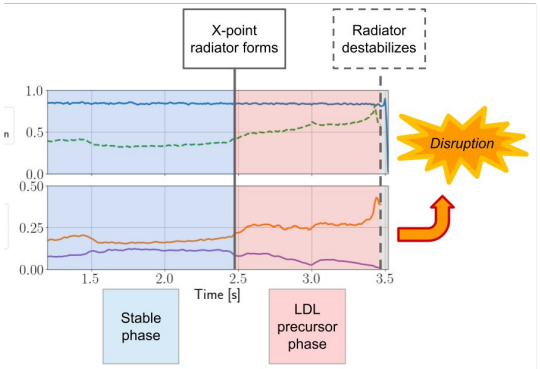

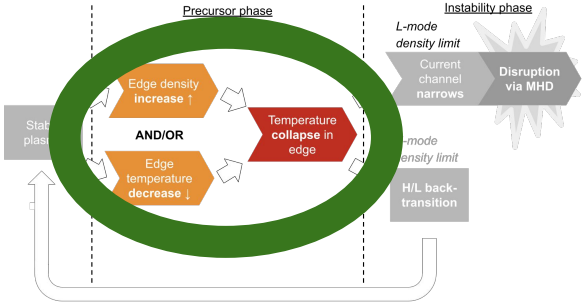

Andrew Maris, maris@mit.edu / 2024-09-03

LSVM classifier finds more accurate stability boundary using edge density and temperature

Model	Analytic boundary	AUC	FPR @ TPR = 95%
Greenwald	$\bar{n}^{\text{limit}} \sim \frac{I_p}{\pi a^2}$	0.971	13.4%
LSVM, edge parameters	$n_{\text{edge}}^{\text{limit}} \sim \frac{I_p^{0.79}}{a^{1.30}} T_{\text{edge}}^{1.00}$	**0.996**	**2.3%**

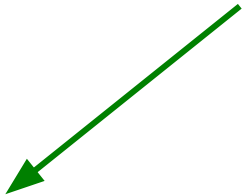

6x fewer false positives!

Andrew Maris, maris@mit.edu / 2024-09-03

LSVM also finds reliable boundary using dimensionless parameters

Model	Analytic boundary	AUC	FPR @ TPR = 95%
Greenwald	$\bar{n}^{\text{limit}} \sim \frac{I_p}{\pi a^2}$	0.971	13.4%
LSVM, edge parameters	$n_{\text{edge}}^{\text{limit}} \sim \frac{I_p^{0.79}}{a^{1.30}} T_{\text{edge}}^{1.00}$	0.996	**2.3%**
LSVM, dimensionless	$\nu_{*,\text{edge}}^{\text{limit}} \sim \beta_{T,\text{edge}}^{-0.40}$	**0.997**	**2.3%**

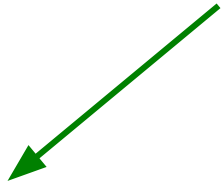

Similarly strong performance

Andrew Maris, maris@mit.edu / 2024-09-03

Boundary using edge parameters achieves strong separation of stable and LDL precursor states

Improved prediction via LDL precursor risk metric

$$\nu_{*,\mathrm{edge}}\beta_{T,\mathrm{edge}}^{0.4}$$

where ν_* is effective collisionality β_T is normalized plasma pressure

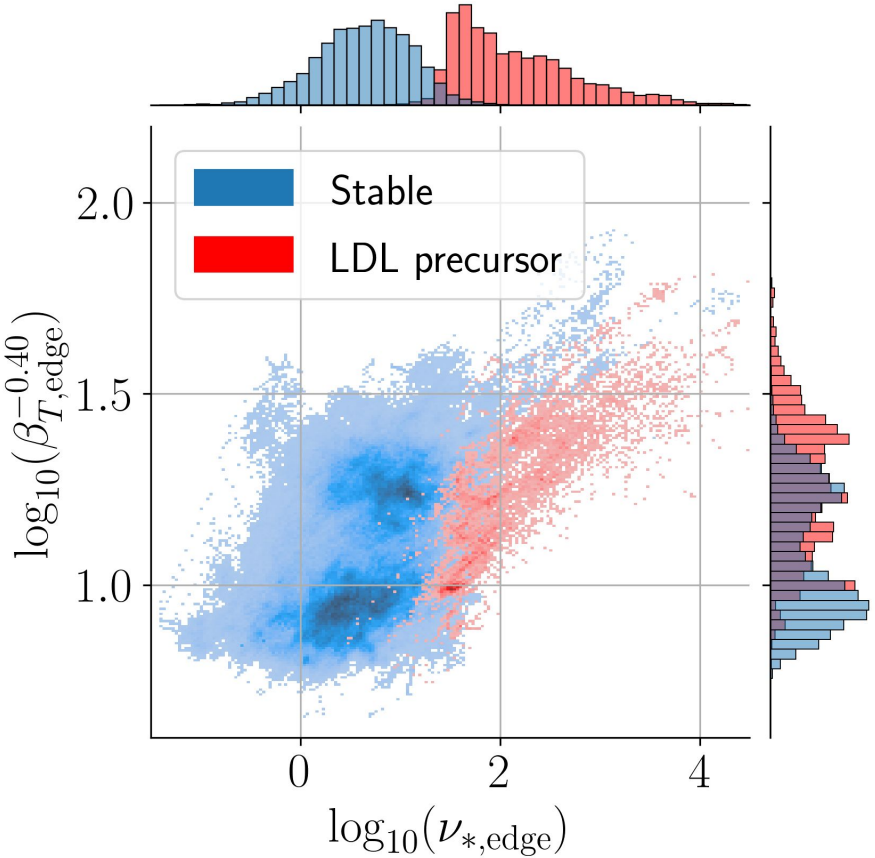

Andrew Maris, maris@mit.edu / 2024-09-03

LDL precursor (LDL-P) risk more reliable than Greenwald fraction at discriminating LDL

Greenwald fraction

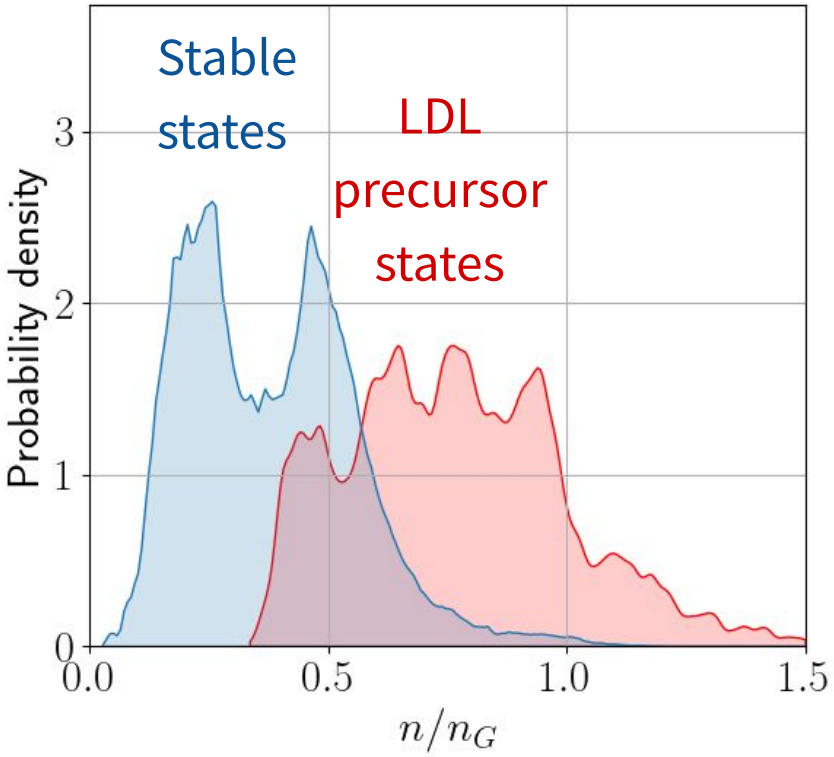

LDL-P risk

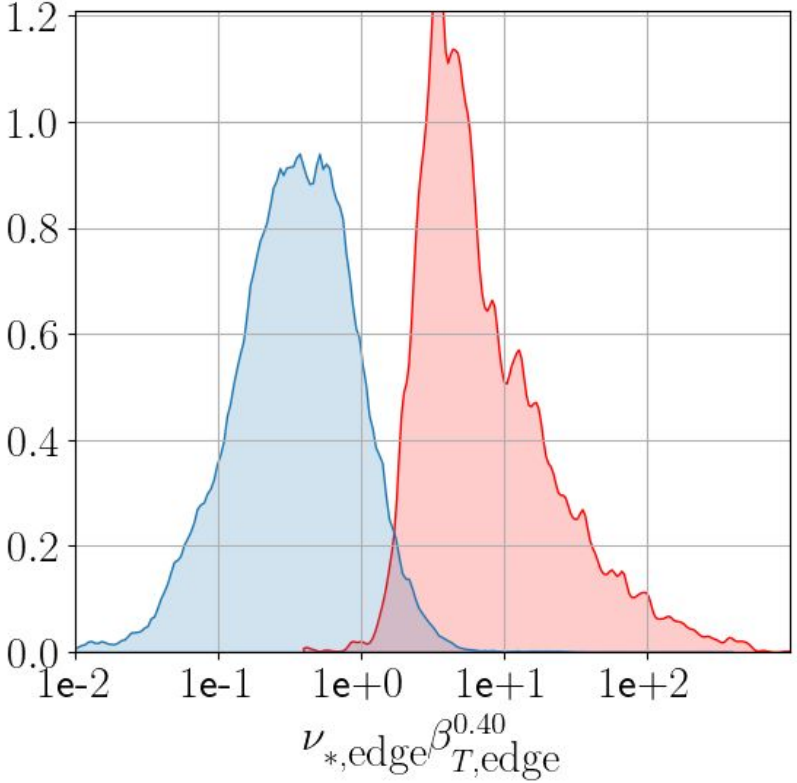

Outline

1. Introduction
2. Description of database
3. Model development
4. **Real-time LDL avoidance at DIII-D**
5. Summary & conclusion

LDL-P risk utilized at DIII-D for real-time LDL avoidance

Real-time Thomson and EFIT

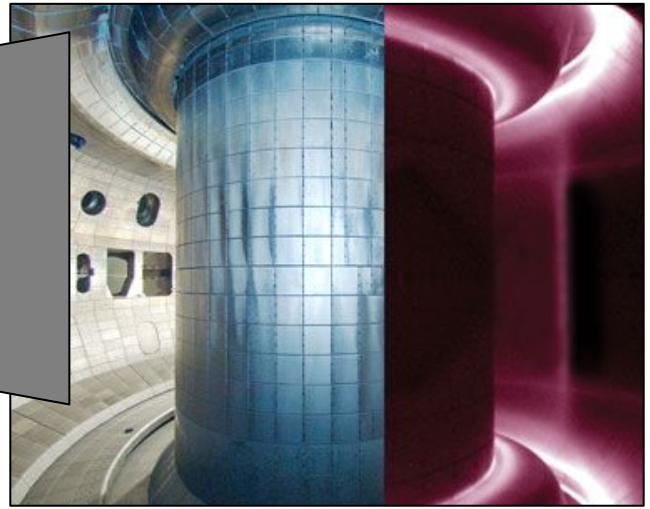

Andrew Maris, maris@mit.edu / 2024-09-03

LDL-P risk utilized at DIII-D for real-time LDL avoidance

Real-time Thomson and EFIT

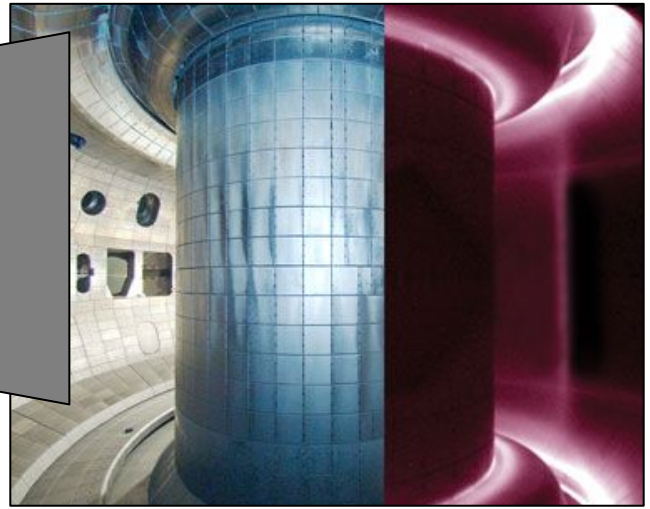

STATIN algorithm
computes
$\nu_{*,\mathrm{edge}}\beta_{T,\mathrm{edge}}^{0.4}$

Andrew Maris, maris@mit.edu / 2024-09-03

LDL-P risk utilized at DIII-D for real-time LDL avoidance

Real-time Thomson and EFIT

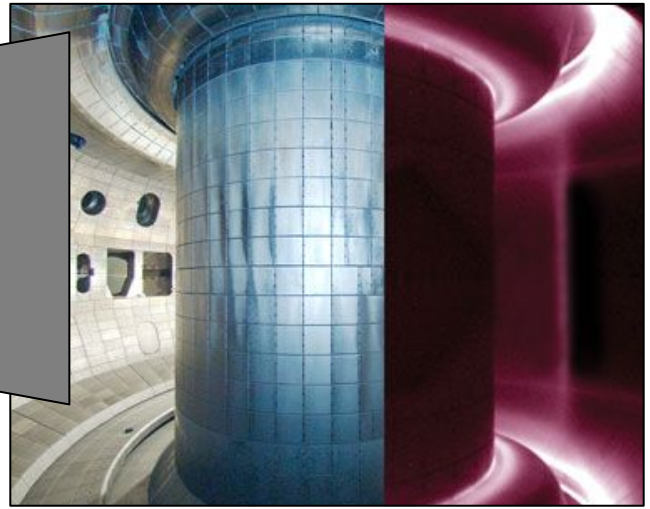

STATIN algorithm computes $\nu_{*,\mathrm{edge}}\beta_{T,\mathrm{edge}}^{0.4}$

LDL-P risk

Proximity Controller or **ONFR**

Andrew Maris, maris@mit.edu / 2024-09-03

LDL-P risk utilized at DIII-D for real-time LDL avoidance

Real-time Thomson and EFIT

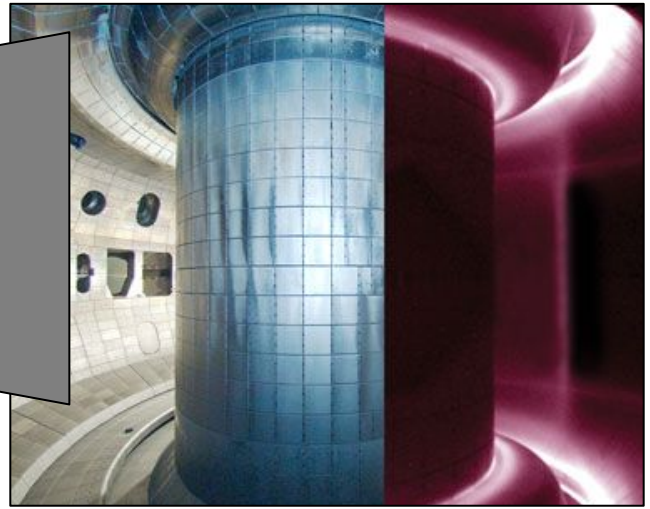

Input power

Density

When risk > threshold

STATIN algorithm computes $\nu_{*,\mathrm{edge}}\beta_{T,\mathrm{edge}}^{0.4}$

LDL-P risk

Proximity Controller or **ONFR**

Andrew Maris, maris@mit.edu / 2024-09-03

LDL-P risk utilized at DIII-D for real-time LDL avoidance

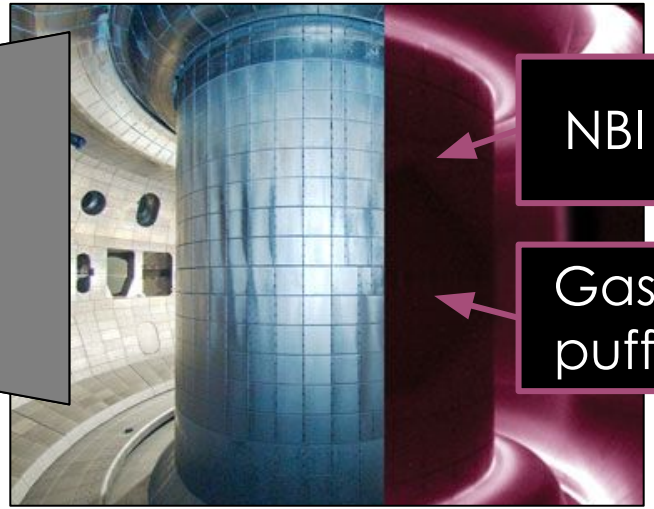

Real-time Thomson and EFIT

NBI

Gas puff

Input power

Density

When risk > threshold

STATIN algorithm computes $\nu_{*,\mathrm{edge}}\beta_{T,\mathrm{edge}}^{0.4}$

LDL-P risk

Proximity Controller or **ONFR**

Avoided LDLs in 16 of 17 shots with controller ON by reducing density & increasing power based on LDL-P risk

199908 - Controller OFF
→ LDL 💥

199909 - Controller ON
→ Stable ✅

LDL-P risk regulated at low value

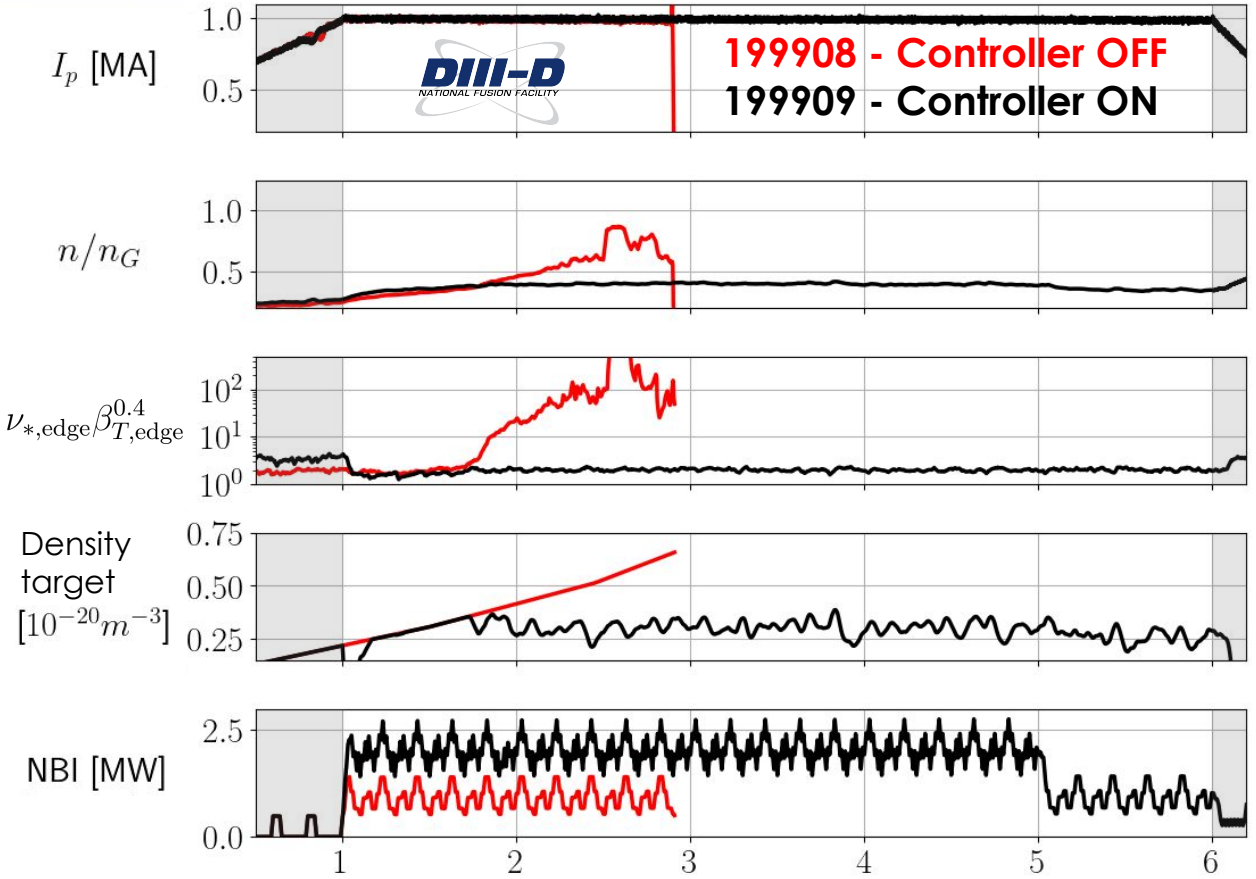

Controller enabled development of stable, gas fueled L-mode reaching Greenwald limit

199908: Controller OFF
- → LDL 💥
- → MARFE @ n/nG ~ 0.6

199921: Controller ON
- → Stable ✅
- → n/nG ~ 1 ✅
- → High LDL-P risk w/out LDL ❔

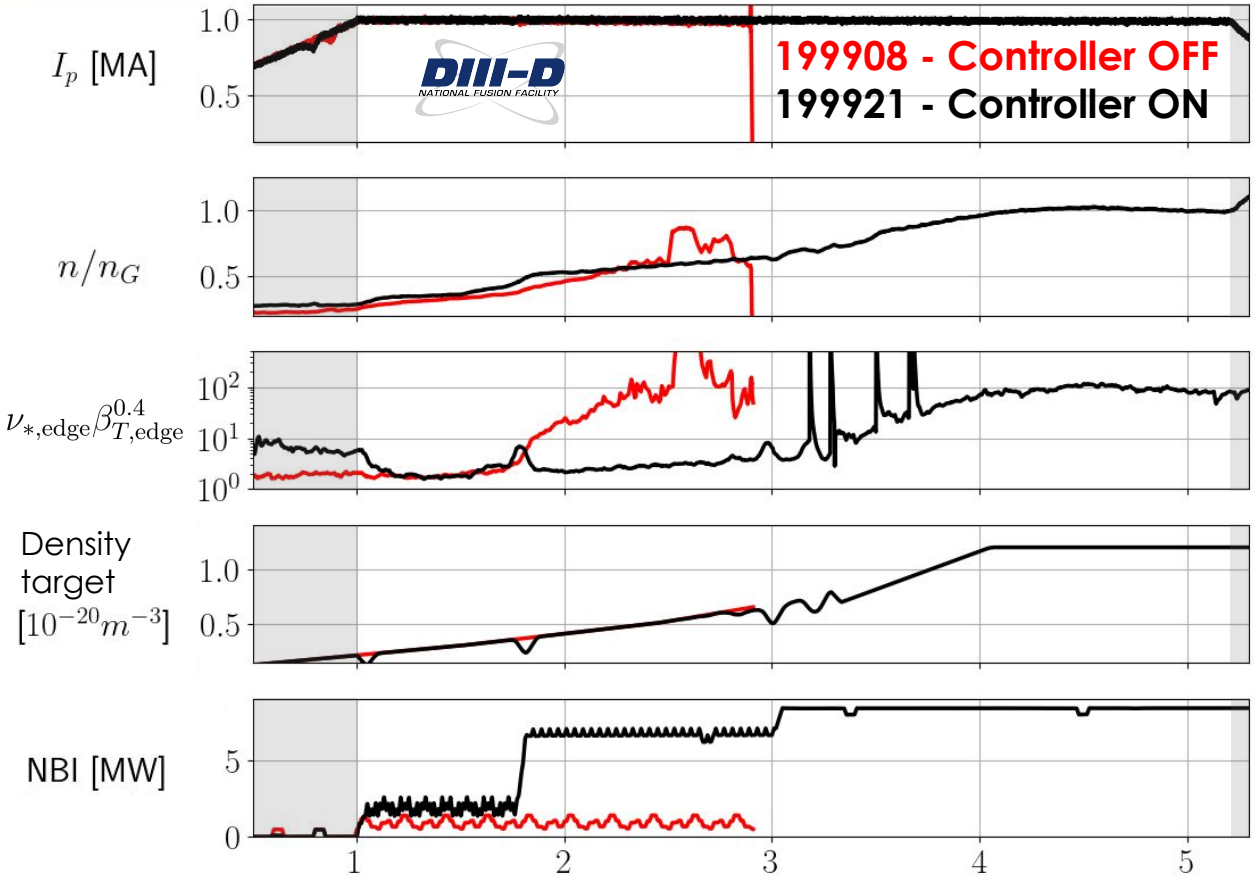

Density limits have been observed to correlate with upper limit on l_i/q_{95}

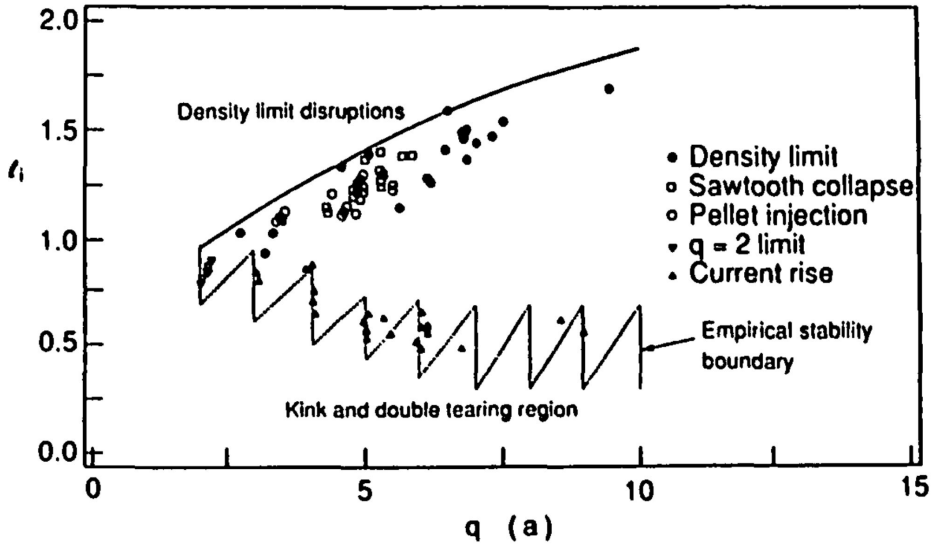

[13]Wesson et al. *NF* 1989

Control experiment sessions
including reference LDLs

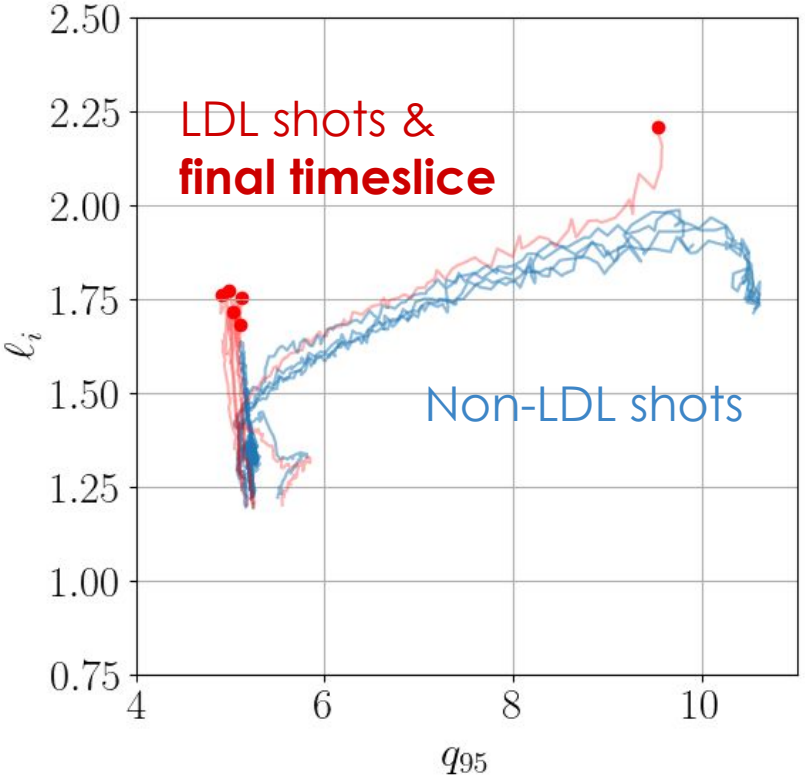

Andrew Maris, maris@mit.edu / 2

Survival at high LDL risk may be due to MHD stability

[14] Cheng et al. *PPCF* 1987

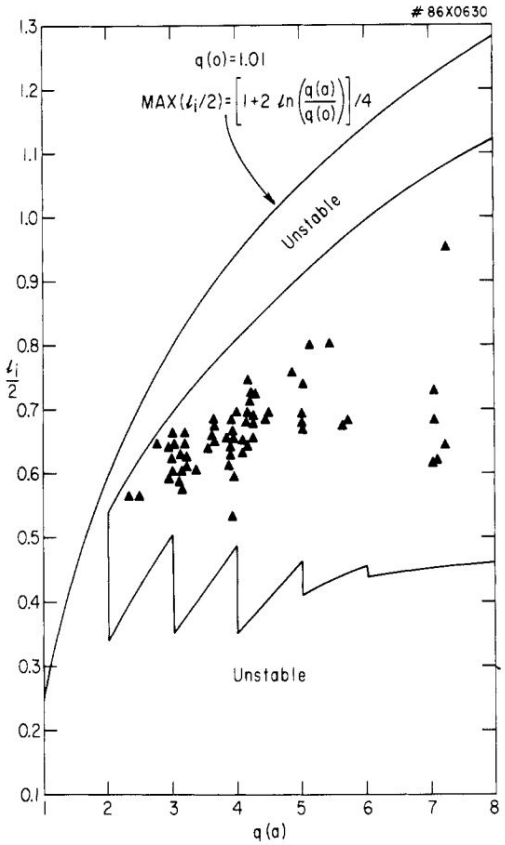

Control experiment sessions
including reference LDLs

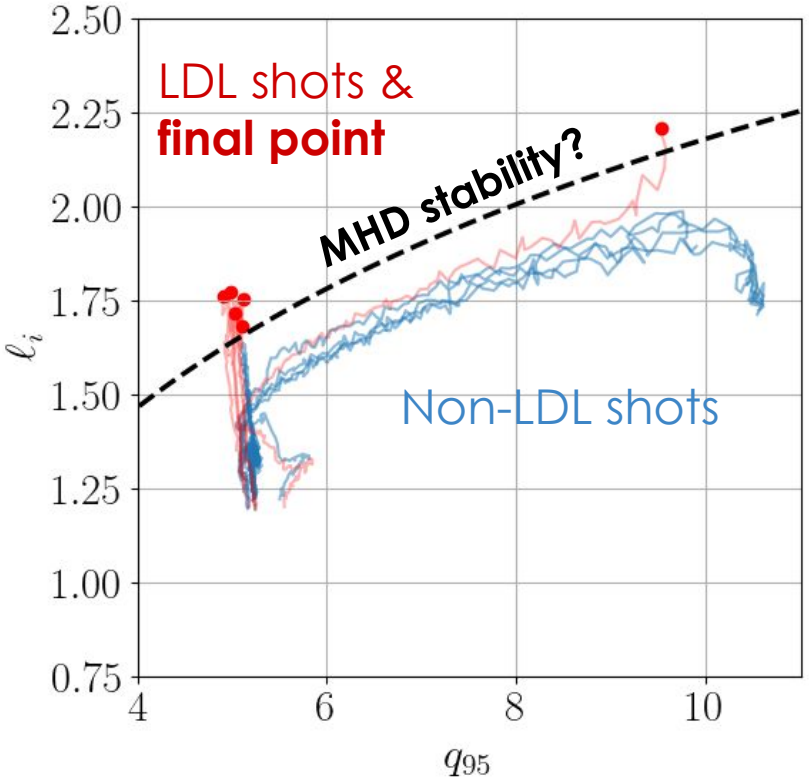

Andrew Maris, maris@

Outline

1. Introduction
2. Description of database
3. Model development
4. Real-time LDL avoidance at DIII-D
5. **Summary & conclusion**

Andrew Maris, maris@mit.edu / 2024-09-03

Multi-machine database & data-driven techniques uncover reliable L-mode density limit precursor (LDL-P) risk metric [1]

- **Two-parameter scaling robustly predicts LDL across devices**

$$\nu_{*,\mathrm{edge}}\beta_{T,\mathrm{edge}}^{0.4}$$ → *good for burning plasmas!*

  - 6x fewer false positives than Greenwald fraction

- **LDL-P risk metric deployed on DIII-D & utilized for successful real-time LDL avoidance (16x)**

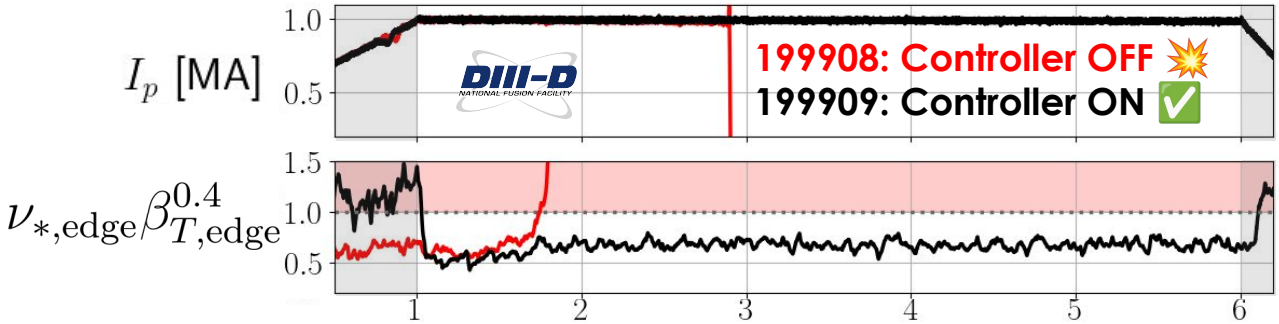

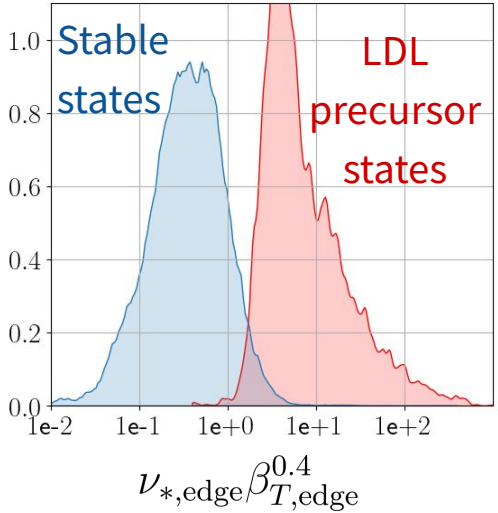

ASDEX Upgrade · Alcator C-Mod · DIII-D · TCV

[1] Maris et al., *Submitted, NF* (2024)

Additional slides

Greenwald fraction does not clearly separate precursor and stable plasma states

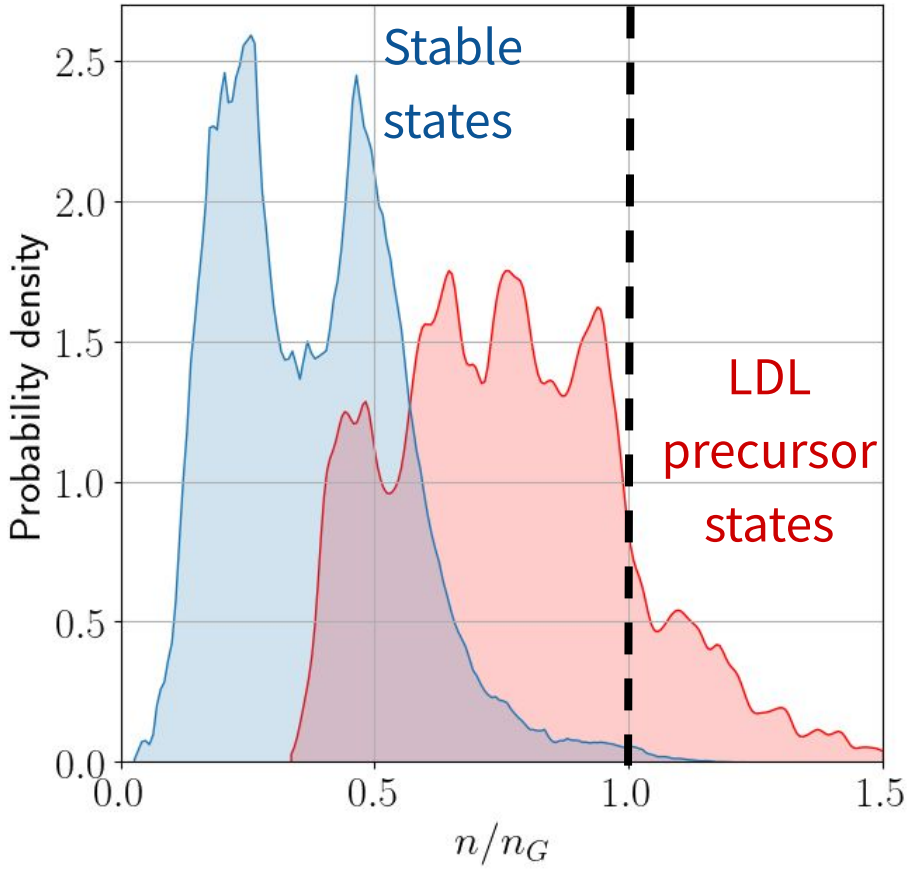

Andrew Maris, maris@mit.edu / 2024-09-03

LDL precursor (LDL-P) risk more reliable than Greenwald fraction at discriminating LDL

Greenwald fraction

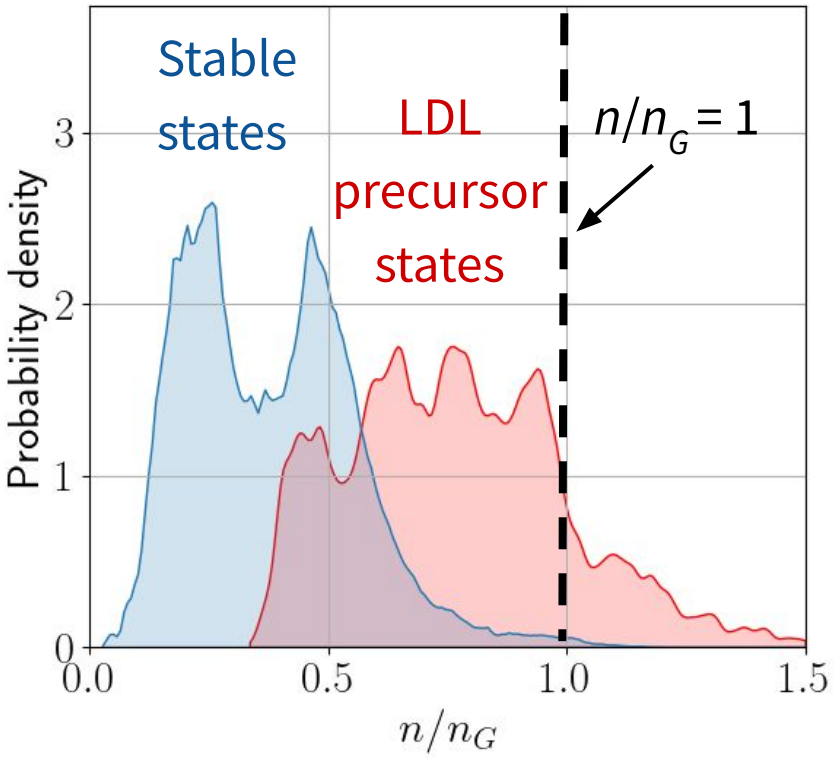

LDL-P risk

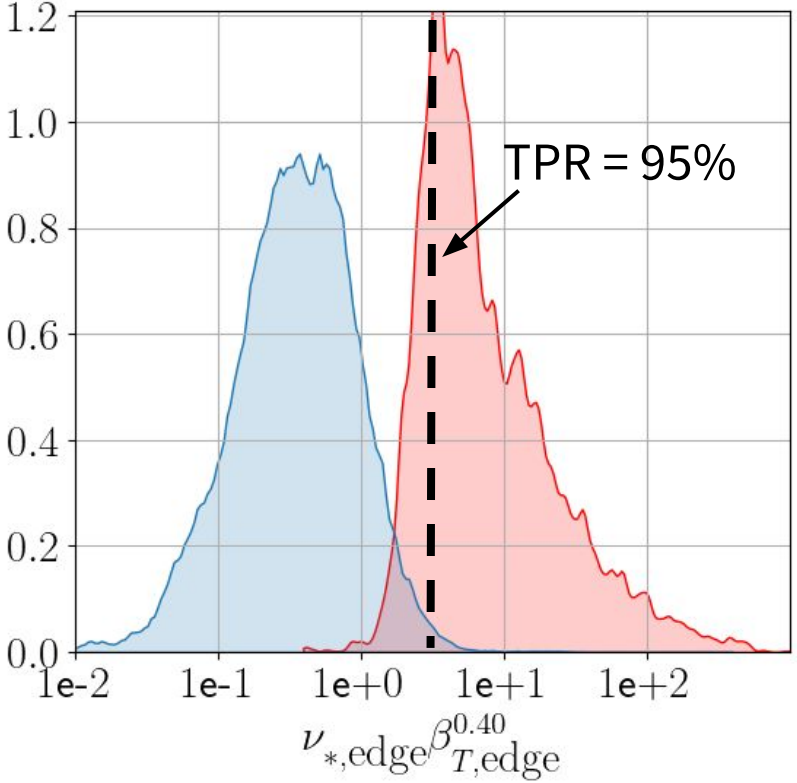

Consider an plasma that enters an unstable phase

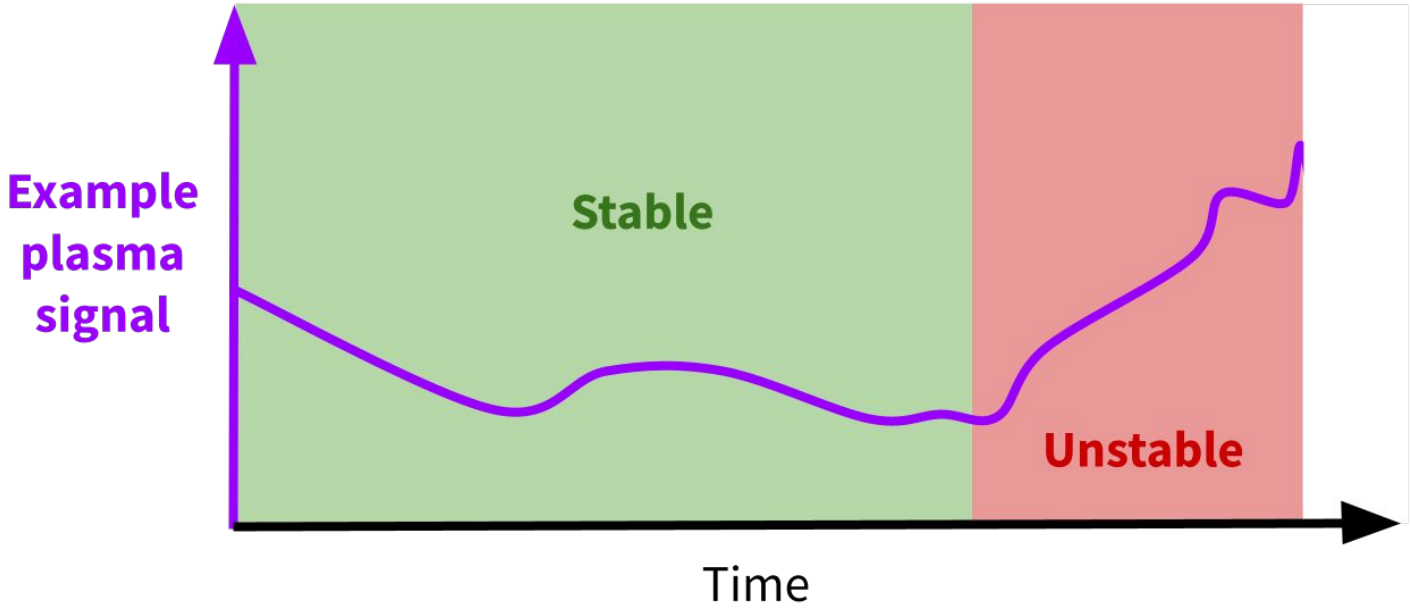

Intuitively, we want our instability predictor to go from low to high when an instability emerges

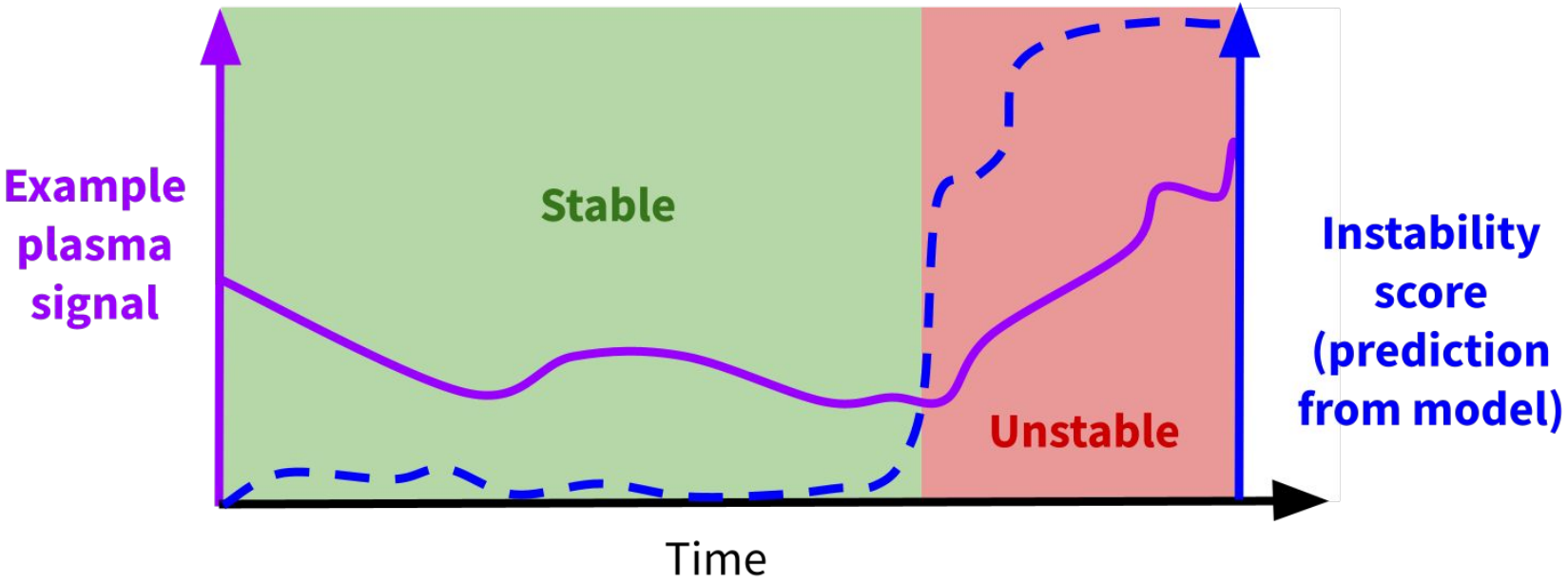

We use an alarm threshold to map instability score "yes/no" warning

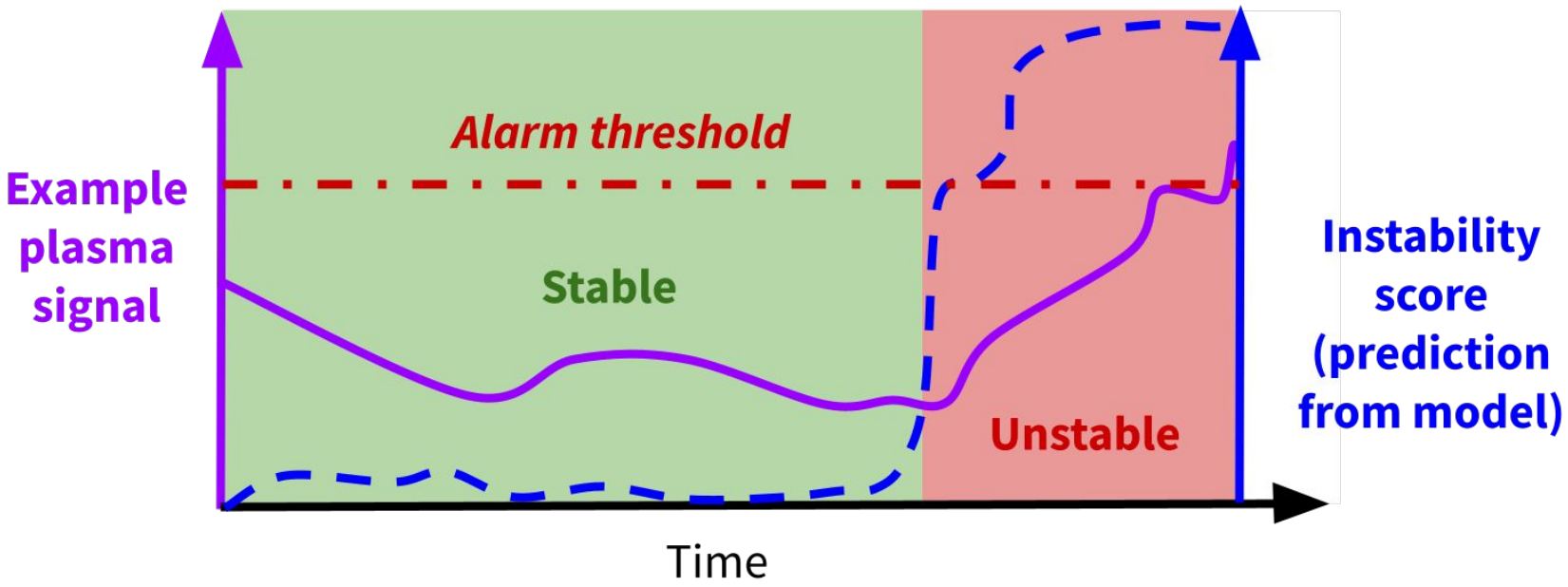

We use an alarm threshold to map instability score "yes/no" warning… this results in an extra degree of freedom

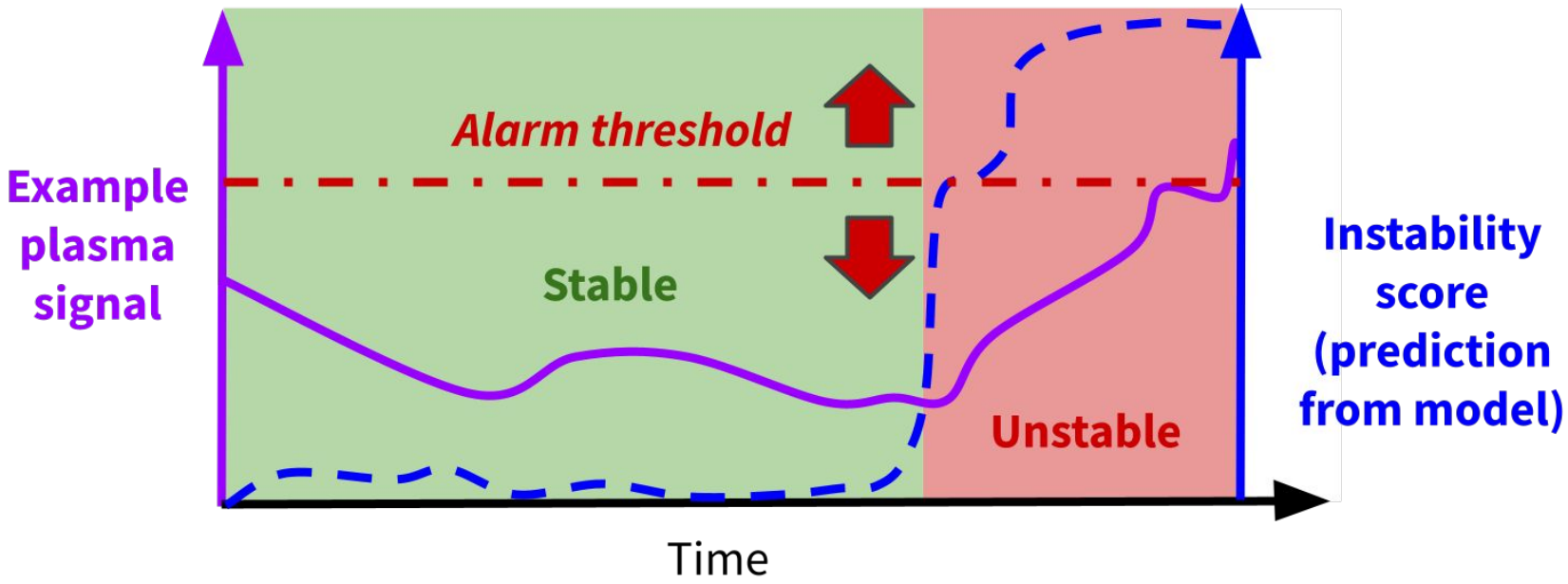

We will compare the Greenwald limit with data-driven density limit predictors

Standard Machine Learning

1. Random forest
2. Neural network

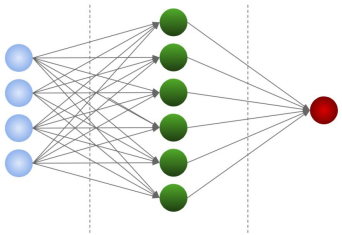

Source: Malato, "How many…" *yourdatateacher.com*

vs.

Analytic/ "Symbolic"

1. Linear Regression
2. Support Vector Machine

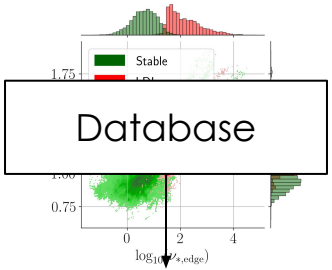

$$\nu_{*,\mathrm{edge}}\beta_{T,\mathrm{edge}}^{0.4}$$

vs.

Greenwald fraction

$$\frac{\bar{n}}{I_p/\pi a^2}$$

We also hypothesize that classification will better identify DL boundary than regression

Linear regression **uses only unstable data**

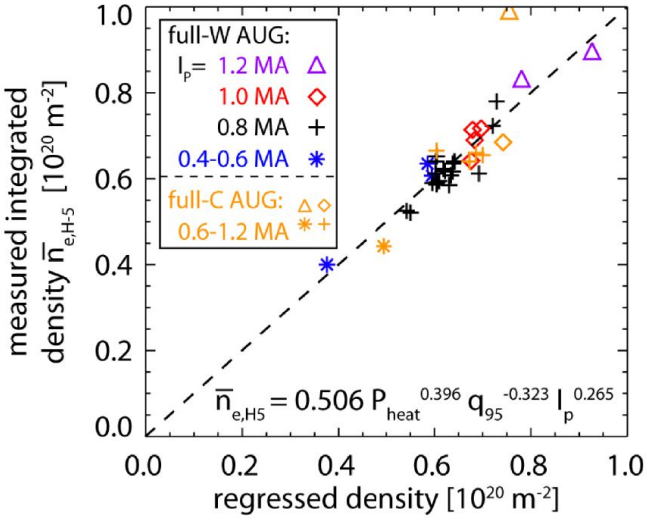

[15] Bernert et al., PPCF (2014)

Classification **uses both stable & unstable data (Linear Support Vector Machine)**

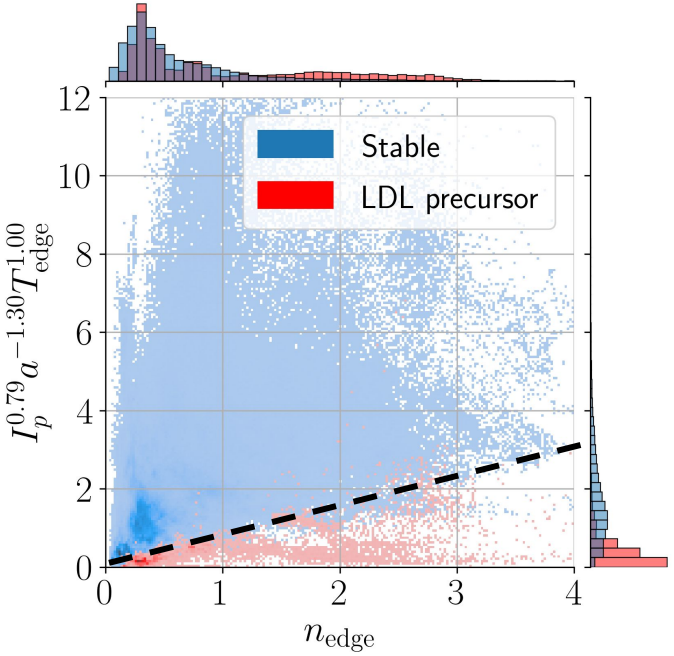

Using global features & EAST data: ML methods achieve significantly higher performance, but still below ITER's needs

Model	Analytic boundary	AUC	FPR @ TPR = 95%
NN	N/A	**0.943**	28.4%
RF	N/A	**0.943**	**22.6%**
LSVM	$\bar{n}^{\text{limit}} \sim \frac{I_p^{0.67}}{a^{1.80}} P_{\text{in}}^{0.28}$	0.941	26.8%
Lin. Reg.	$\bar{n}^{\text{limit}} \sim \frac{I_p^{0.75}}{a^{2.04}} P_{\text{in}}^{0.17}$	0.925	39.5%
Greenwald	$\bar{n}^{\text{limit}} \sim \frac{I_p}{\pi a^2}$	0.894	46.0%

Using edge features: significantly improved density limit prediction accuracy achieved by NN, RF and LSVM

Model	Analytic boundary	AUC	FPR @ TPR = 95%
NN	N/A	0.997	2.8%
RF	N/A	**0.998**	**0.5%**
LSVM	$n_{\text{edge}}^{\text{limit}} \sim \frac{I_p^{0.79}}{a^{1.30}} T_{\text{edge}}^{1.00}$	0.996	2.3%
Lin. Reg.	$n_{\text{edge}}^{\text{limit}} \sim \frac{I_p^{0.86}}{a^{1.48}} T_{\text{edge}}^{0.11} q_{95}^{0.66}$	0.880	54.6%
Greenwald	$\bar{n}^{\text{limit}} \sim \frac{I_p}{\pi a^2}$	0.971	13.9%
Edge Greenwald	$n_{\text{edge}}^{\text{limit}} \sim \frac{I_p}{\pi a^2}$	0.888	43.7%

Four-parameter power-law identified by LSVM comparable accuracy to far more sophisticated NN & RF

Using dimensionless features: similarly strong performance from data-driven models

Model	Analytic boundary	AUC	FPR @ TPR = 95%
NN	N/A	0.991	3.0%
RF	N/A	0.996	**1.6%**
LSVM	$\nu^{\text{limit}}_{*,\text{edge}} \sim \beta^{-0.40}_{T,\text{edge}}$	**0.997**	2.3%
Lin. Reg.	$\nu^{\text{limit}}_{*,\text{edge}} \sim \beta^{-0.67}_{T,\text{edge}} \rho^{-0.77}_{*,\text{edge}}$	0.984	6.6%
Greenwald	$\bar{n}^{\text{limit}} \sim \frac{I_p}{\pi a^2}$	0.971	13.9%
Edge Greenwald	$n^{\text{limit}}_{\text{edge}} \sim \frac{I_p}{\pi a^2}$	0.888	43.7%

Andrew Maris, maris@mit.edu / 2024-09-03

Average value and standard deviation of global parameters for each device in the database

Device	n_e [10^{20} m^{-3}]	I_p [MA]	a [m]	R_0 [m]	B_T [T]	P_{in} [MW]
AUG	0.68 ± 0.16	0.72 ± 0.13	0.50 ± 0.01	1.60 ± 0.01	2.41 ± 0.23	6.61 ± 1.66
C-Mod	1.45 ± 0.68	0.83 ± 0.18	0.22 ± 0.00	0.68 ± 0.00	5.44 ± 0.81	1.73 ± 1.05
DIII-D	0.44 ± 0.17	1.04 ± 0.21	0.59 ± 0.02	1.67 ± 0.00	1.94 ± 0.17	5.87 ± 3.17
EAST	0.33 ± 0.09	0.35 ± 0.06	0.44 ± 0.01	1.83 ± 0.00	2.43 ± 0.00	3.29 ± 1.77
TCV	0.47 ± 0.20	0.18 ± 0.07	0.23 ± 0.01	0.88 ± 0.01	1.42 ± 0.03	0.57 ± 0.49

Average value and standard deviation of several dimensionless parameters in the edge of the plasma

Device	q_{95}	$\nu_{*,\mathrm{edge}}$	$\beta_{T,\mathrm{edge}}$ [%]	ρ^*_{edge} [%]
AUG	6.00 ± 0.97	16.51 ± 73.24	0.42 ± 0.17	0.37 ± 0.07
C-Mod	4.53 ± 0.96	19.97 ± 272.04	0.16 ± 0.16	0.38 ± 0.10
DIII-D	5.08 ± 1.48	3.69 ± 18.74	0.67 ± 0.39	0.51 ± 0.14
EAST	7.97 ± 1.29	N/A	N/A	N/A
TCV	4.85 ± 1.19	52.53 ± 72.99	0.19 ± 0.17	0.77 ± 0.23

Applying same approach when training on all devices and testing on DIII-D

Model	Analytic boundary	AUC	FPR @ TPR = 95%
NN	N/A	0.987	3.3%
RF	N/A	**0.995**	**1.5%**
LSVM	$\nu^{\text{limit}}_{*,\text{edge}} \sim \beta^{-0.41}_{T,\text{edge}}$	0.992	1.6%
Lin. Reg.	$\nu^{\text{limit}}_{*,\text{edge}} \beta^{-1.06}_{T,\text{edge}}$	0.974	9.6%
Greenwald	$\bar{n}^{\text{limit}} \sim \frac{I_p}{\pi a^2}$	0.847	53.7%
Edge Greenwald	$n^{\text{limit}}_{\text{edge}} \sim \frac{I_p}{\pi a^2}$	0.705	82.6%

Comparing with Giacomin-Ricci scaling shows greater prediction performance for collisionality-like boundary

Model	Analytic boundary	AUC	FPR @ TPR = 95%
NN	N/A	0.984	6.4%
RF	N/A	0.985	**3.0%**
LSVM	$\nu^{\text{limit}}_{*,\text{edge}} \sim \beta^{-0.41}_{T,\text{edge}}$	**0.992**	3.5%
Lin. Reg.	$\nu^{\text{limit}}_{*,\text{edge}} \sim \beta^{-1.14}_{T,\text{edge}}$	0.976	11.4%
Giacomin	$n^{\text{limit}}_{\text{edge}} \sim \frac{I_p^{22/21}}{a^{79/42}} \frac{P_{SOL}^{10/21} A^{1/6} R_0^{1/42}}{B_T^{8/21}(1+\kappa^2)^{1/3}}$	0.915	22.8%
Greenwald	$\bar{n}^{\text{limit}} \sim \frac{I_p}{\pi a^2}$	0.896	44.1%
Edge Greenwald	$n^{\text{limit}}_{\text{edge}} \sim \frac{I_p}{\pi a^2}$	0.745	79.2%

Only AUG, TCV, and DIII-D, as P_{SOL} could not be estimated for C-Mod database

SVM identifies edge collisionality-like scaling

Edge density limit scaling

$$n_{\text{edge}}^{\text{limit}} \sim \frac{I_p^{0.8}}{a^{1.3}} T_{\text{edge}}^{1.0}$$

achieves strong separation of cases

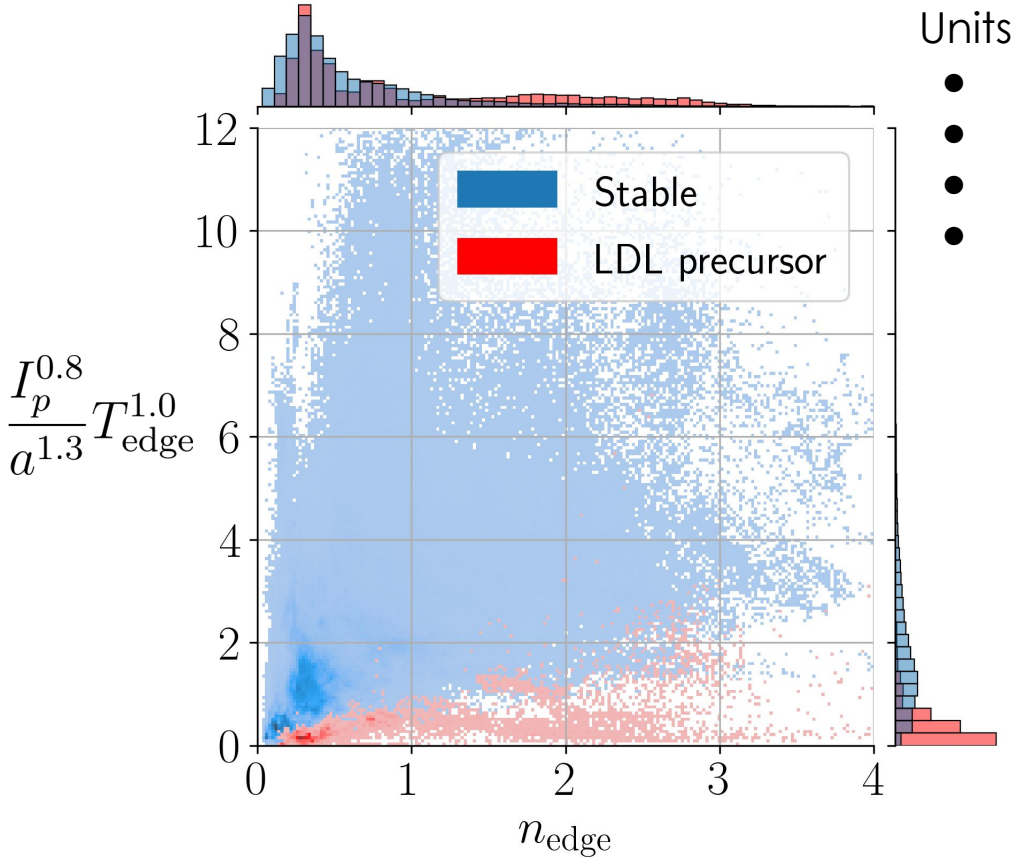

Units:

- 10^{20} m^{-3}
- MA
- m
- keV

Andrew Maris, maris@mit.edu / 2024-09-03

Stability boundary connected to enhanced transport and XPR/MARFE instability

Enhanced turbulence theories [17, 18] often point to electron adiabaticity

$$\alpha \equiv \frac{k_{||}^2 v_{te}^2}{\nu_{ee}\omega}$$

Collisionality boundary is close match to adiabaticity, with implied turbulence frequency

$$\omega_{\text{implied}} = \frac{T_{\text{edge}}^{0.9}}{B_T^{0.8}} \frac{n_{\text{edge}}^{0.4} k_{||}}{\epsilon^{3/2}}$$

XPR/MARFE instability model model [19] (assuming $n_0 \sim n_{sep}$ as in [16]) has similar T dependence

$$n_{\text{edge}}^{\text{limit}} \sim \frac{T_{\text{edge}}^{5/4}\sqrt{a}}{q_s R_0}$$

although geometric factors differ

[16] Manz and Eich, NF (2023)
[17] Rogers et al., PRL (1998)
[18] Diamond et al., Phil. Trans. A. (2023)
[19] Stroth et al., NF (2022)

Andrew Maris, maris@mit.edu / 2024-09-03

LDL also avoided in current ramp-down scenario

199586: Controller OFF
→ LDL 💥
199587: Controller ON
→ Stable ✅

Relatively high n/n_G achieved without disruption

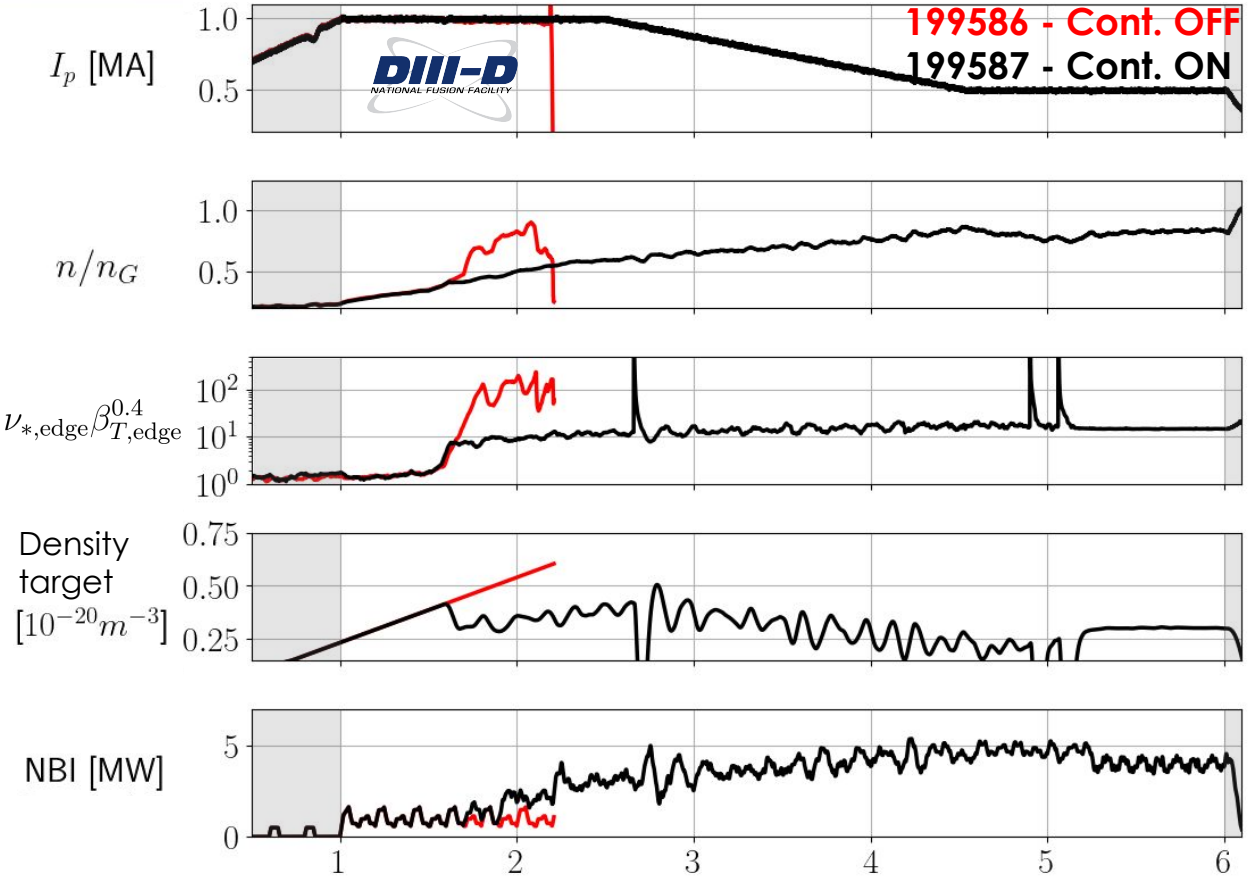

Example of successful prediction: DIII-D 191793

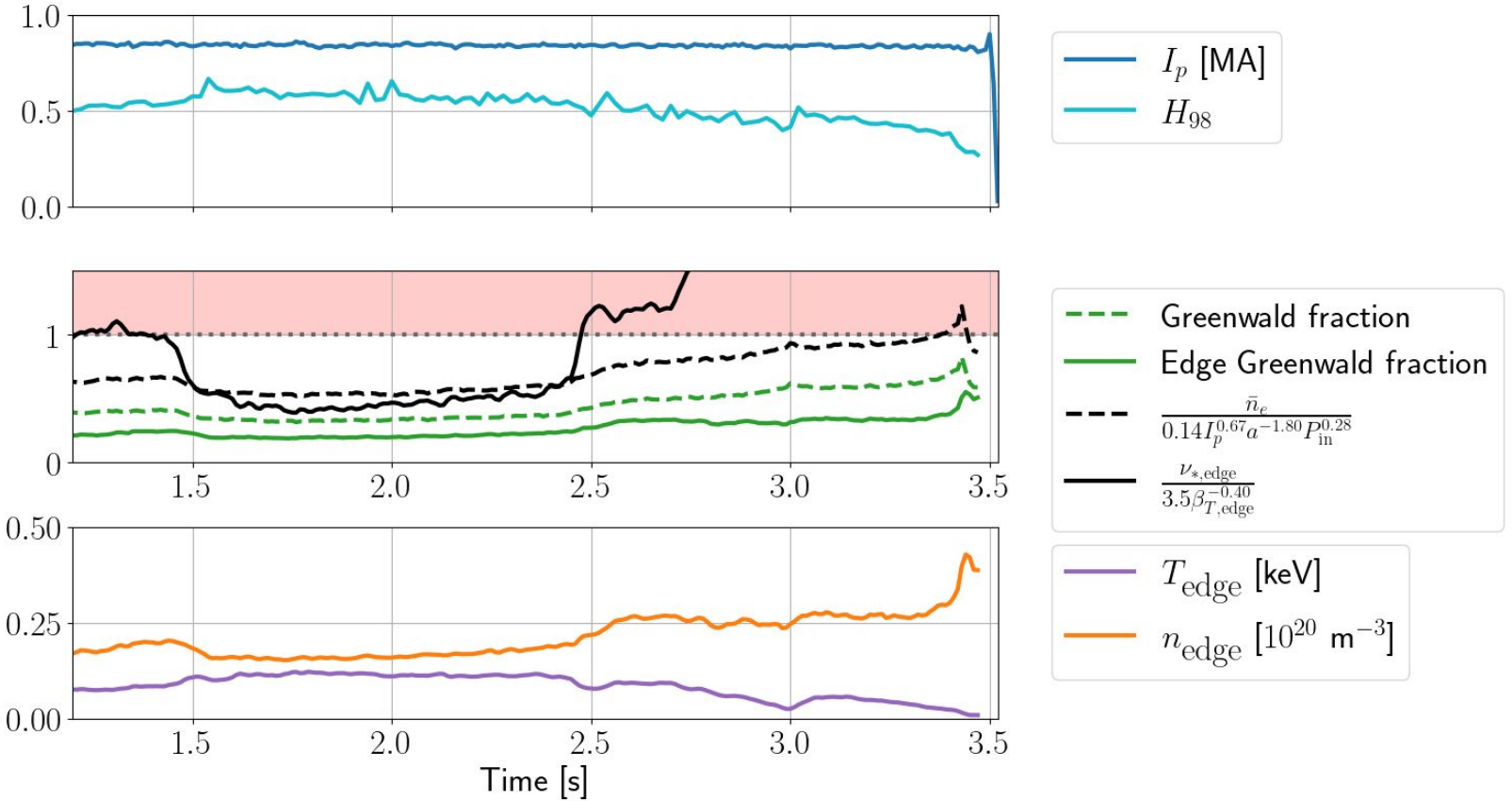

Additionally, we will consider different sets of "features" to train the models on

Symbol	Definition	"Global" features	"Edge" features	Dimensionless features
$\bar{n}$	e^- density, line avg.	X		
P_{in}	Input power	X		
n_{edge}	e^- density, edge		X	
T_{edge}	e^- temperature, edge		X	
I_p	Plasma current	X	X	
a	Minor radius	X	X	
q_{95}	Safety factor		X	X
$\nu_{*,\text{edge}}$	Collisionality, edge			X
$\beta_{T,\text{edge}}$	Toroidal β, edge			X
$\rho^{*,\text{edge}}$	Norm. gyroradius, edge			X

This dimensionless boundary is nearly identical to the "edge" features boundary

Dimensionless LDL boundary:

$$\nu^*_{\text{edge}}\beta^{0.4}_{T,\text{edge}} \longrightarrow \frac{n^{1.4}_{\text{edge}}}{T^{1.6}_{\text{edge}}}\frac{R_0^2 B_T^{0.2}\epsilon^{0.5}\kappa}{I_p} \longrightarrow \frac{n_{\text{edge}}}{T^{1.1}_{\text{edge}}}\frac{a^{1.4}}{I_p^{0.7}}\underbrace{\left(B_T^{0.1}\epsilon^{-0.6}\kappa^{0.7}\right)}$$

Varies weakly in database:
Mean = 3.8
Std dev = 0.44

Edge features LDL boundary:

$$\frac{n_{\text{edge}}}{n_{\text{limit}}} = \frac{n_{\text{edge}}}{T^{1.0}_{\text{edge}}}\frac{a^{1.3}}{I_p^{0.8}}$$

Despite more degrees of freedom in "edge" features case, nearly same boundary found

LDL risk metric can also be used for H-mode DLs (HDLs) on AUG, DIII-D, and TCV

- **HDL database in development, currently at 71 shots**
- **"HDL precursor" here defined as 100ms before HDL (or 30 ms for TCV)**

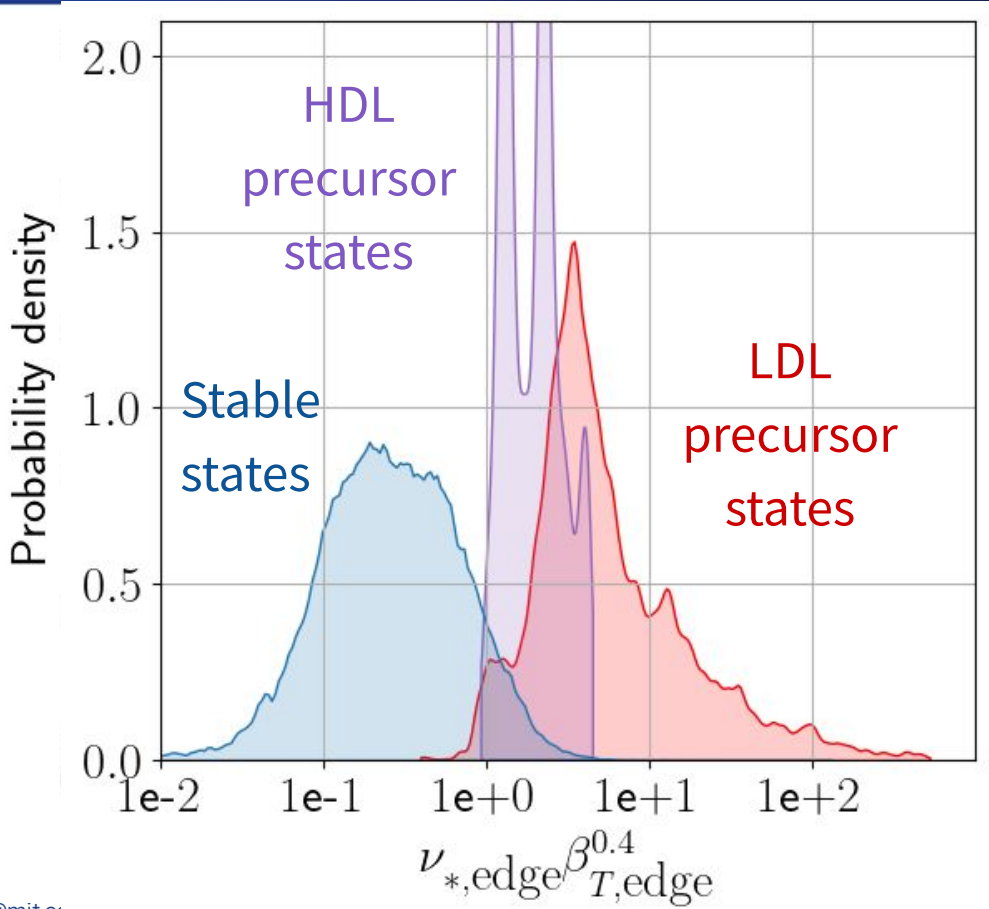

Andrew Maris, maris@mit.e

HDL overlaps with LDL in Greenwald fraction

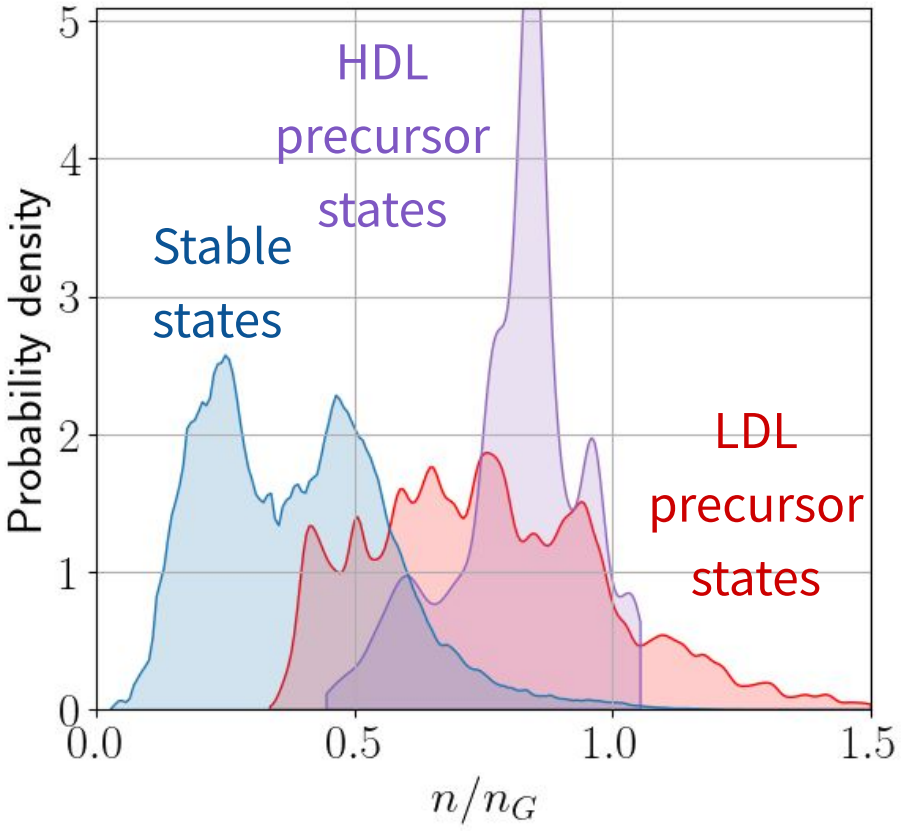

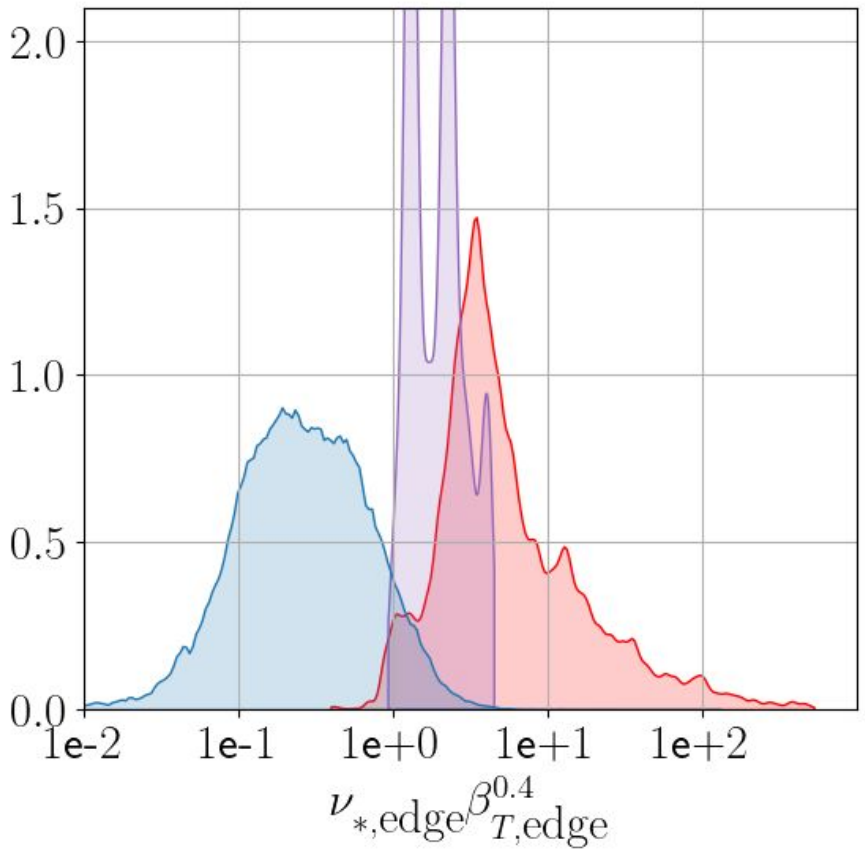

For future devices, LDL risk metric predicts significant safety margins to HDL

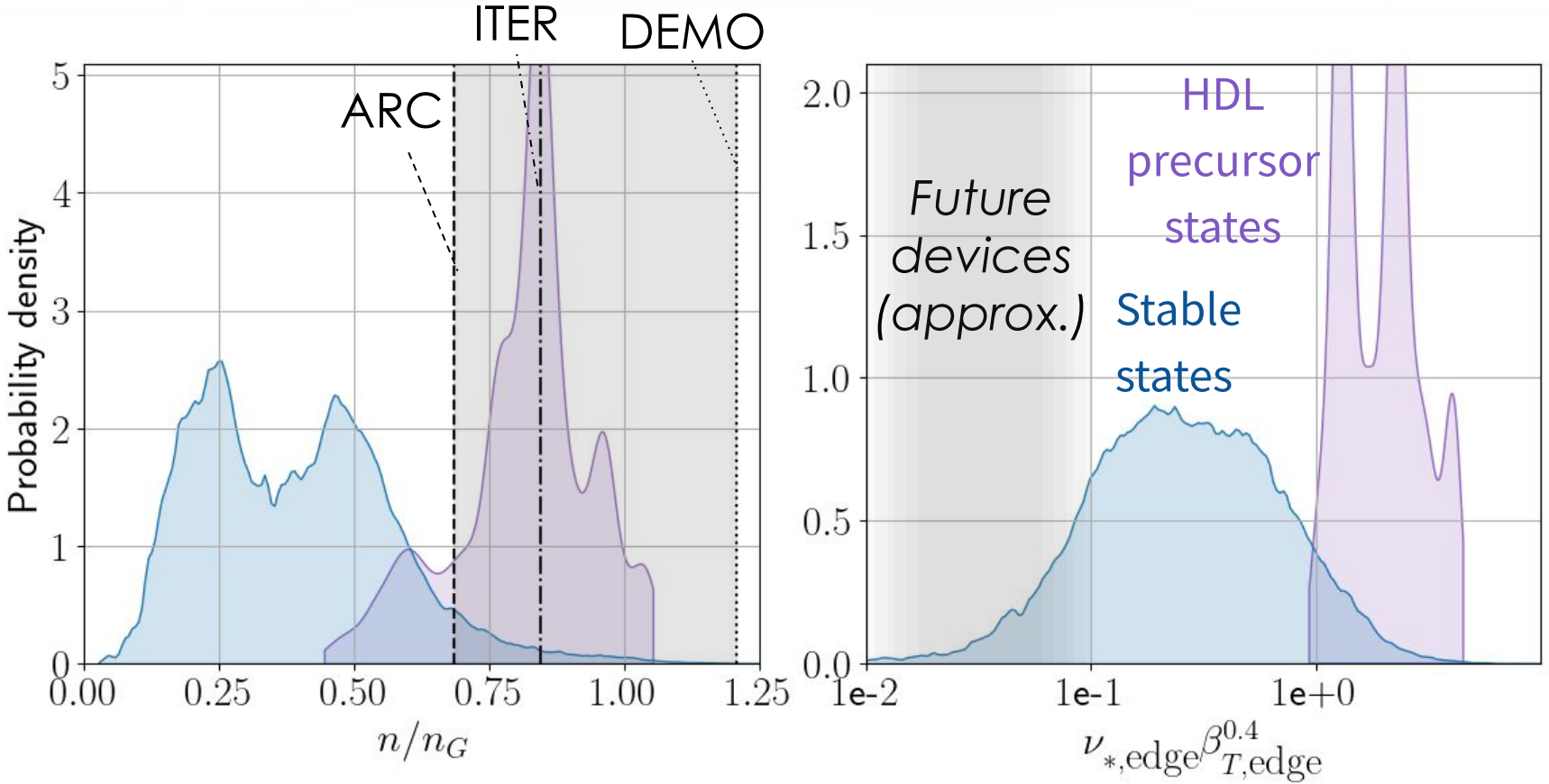

Linear Support Vector Machines (LSVMs) identify boundaries between data classes

- For linearly separable data, LSVM finds boundary that maximizes distance to closest points
- Definition: for *n* data samples $x_i \in \mathbb{R}^d$, *n* labels $y_i \in \{-1,1\}$, vector $w \in \mathbb{R}^d$ normal to boundary, and intercept $b \in \mathbb{R}$, an LSVM minimizes the cost function

$$\mathcal{L} = C\left(\frac{1}{n}\sum_{i=1}^{n}\max\left(0, 1 - y_i(\mathbf{w}^T\mathbf{x}_i - b)\right)\right) + ||\mathbf{w}||^2$$

Incorrect classification penalty — Regularization

with only one hyperparameter, C

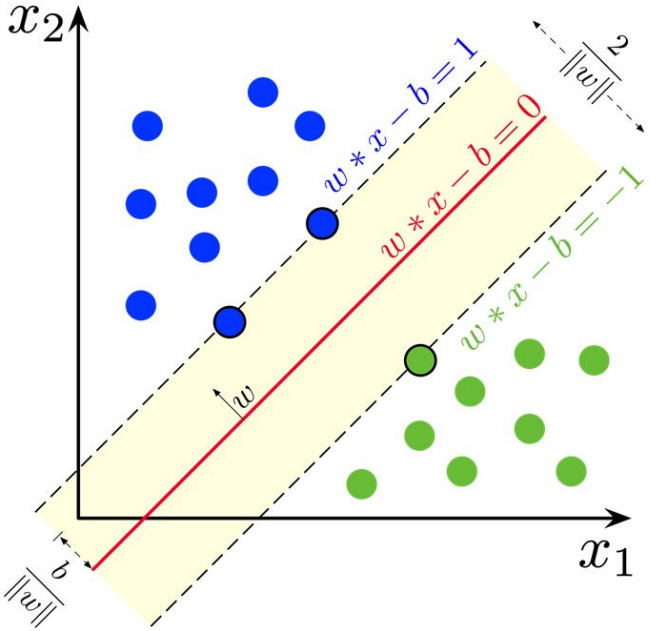

Cartoon of LSVM

Radiator/MARFE movement generally precedes LDL

1) Radiator forms

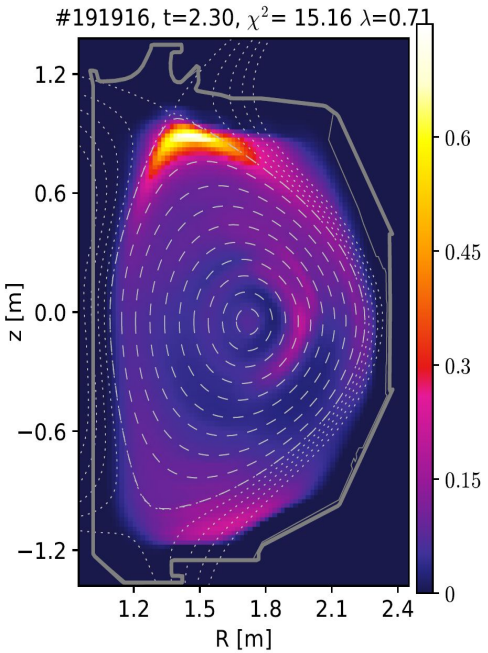

2) Moves toward core

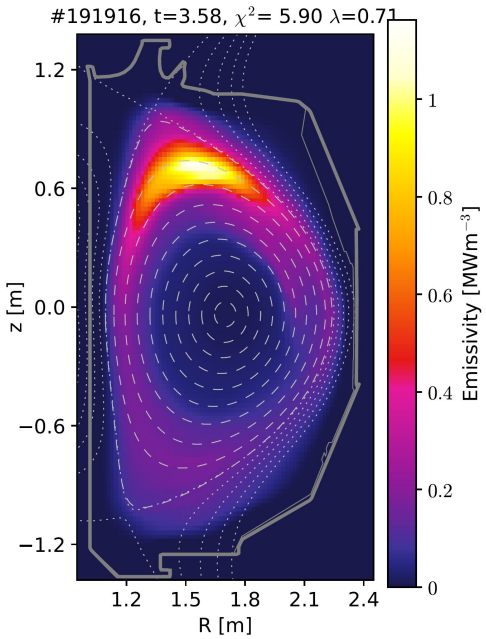

3) Flips position

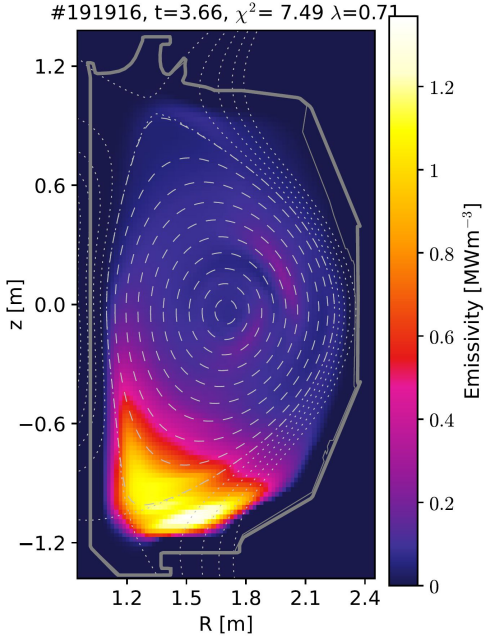

Andrew Maris, maris@mit.edu / 2024-09-03